

Anharmonic free energies and phonon dispersions from the stochastic self-consistent harmonic approximation: application to platinum and palladium hydrides

Ion Errea^{1,2}, Matteo Calandra¹, and Francesco Mauri¹

¹*Université Pierre et Marie Curie-Paris 6, CNRS, IMPMC-UMR7590,
case 115, 4 Place Jussieu, 75252 Paris Cedex 05, France and*

²*IKERBASQUE, Basque Foundation for Science, 48011, Bilbao, Spain*

Harmonic calculations based on density-functional theory are generally the method of choice for the description of phonon spectra of metals and insulators. The inclusion of anharmonic effects is, however, delicate as it relies on perturbation theory requiring a considerable amount of computer time, fast increasing with the cell size. Furthermore, perturbation theory breaks down when the harmonic solution is dynamically unstable or the anharmonic correction of the phonon energies is larger than the harmonic frequencies themselves. We present here a stochastic implementation of the self-consistent harmonic approximation valid to treat anharmonicity at any temperature in the non-perturbative regime. The method is based on the minimization of the free energy with respect to a trial density matrix described by an arbitrary harmonic Hamiltonian. The minimization is performed with respect to all the free parameters in the trial harmonic Hamiltonian, namely, equilibrium positions, phonon frequencies and polarization vectors. The gradient of the free energy is calculated following a stochastic procedure. The method can be used to calculate thermodynamic properties, dynamical properties and even anharmonic corrections to the Eliashberg function of the electron-phonon coupling. The scaling with the system size is greatly improved with respect to perturbation theory. The validity of the method is demonstrated in the strongly anharmonic palladium and platinum hydrides. In both cases we predict a strong anharmonic correction to the harmonic phonon spectra, far beyond the perturbative limit. In palladium hydrides we calculate thermodynamic properties beyond the quasiharmonic approximation, while in PtH we demonstrate that the high superconducting critical temperatures at 100 GPa predicted in previous calculations based on the harmonic approximation are strongly suppressed when anharmonic effects are included.

I. INTRODUCTION

Describing accurately vibrations of atoms is of paramount importance in the physical properties of solids, liquids and molecules. The contribution of atomic vibrations to the free energy of the system affects equilibrium and thermodynamic properties, while the frequencies and the deformation potentials determine transport and superconducting properties. Moreover, the spectra obtained from spectroscopic techniques such as infrared, Raman, and inelastic X-ray or neutron scattering cannot be understood without accounting for atomic vibrations. The quantum mechanical description of atomic vibrations in terms of phonons or vibrons has provided a successful framework to describe all these properties¹.

Nowadays, vibron energies and phonon dispersions in the harmonic approximation are routinely calculated from first-principles making use of linear response theory² or the small displacement method³, and thermodynamic properties can be accounted within the standard quasiharmonic approximation⁴. The harmonic approximation relies on the following assumptions: (i) the displacement of the atoms from their equilibrium positions is small compared to the interatomic distance and, as a consequence, (ii) the ionic potential can be approximated with the truncation at second order of the Born-Oppenheimer (BO) energy surface. The harmonic approximation predicts that phonons or vibrons are well-defined quasiparticles with an infinite lifetime. Thus, finite values of the thermal conductivity in solids cannot

be accounted for. Moreover, harmonic vibrational energies are temperature independent and, therefore, thermodynamic properties at high temperature might not be properly accounted within the harmonic approximation. Despite being computationally challenging for *ab initio* approaches, phonons finite lifetime and the temperature dependence of their frequencies can be explained treating third and fourth order terms in the expansion of the BO energy surface within perturbation theory⁵⁻⁹ at a very high computational cost, fast increasing with the system size.

The validity of perturbation theory is, however, limited to situations in which the harmonic potential is considerably larger than higher order terms. Then, the perturbative correction of vibrational frequencies is small with respect to the harmonic result. Nevertheless, whenever the displacements of the atoms largely exceed the range in which the harmonic potential is valid, the harmonic approximation and any perturbative approach based on it break down^{10,11}. This situation occurs whenever a system is close to a dynamical instability, light atoms are present, or temperature is high and the solid is not far from melting. In these cases, describing the temperature dependence of the phonon spectra is crucial and incorporating anharmonic corrections to the free energy is mandatory to describe properly thermodynamic properties. This non-perturbative regime has already been identified in superconductors¹²⁻¹⁶, transition-metal dichalcogenides with charge-density waves¹⁷⁻²¹, thermoelectric materials²², ferroelectrics^{23,24}, hydrides²⁵, materials un-

der extreme temperature or pressure conditions^{26–28}, or in the isotopic fractionation of water²⁹ to mention but a few examples. The development of a non-perturbative treatment of phonon-phonon scattering is thus a major challenge for many fields of physics and chemistry.

Ab initio molecular dynamics (AIMD)³⁰ calculations are the most common way of treating anharmonicity at any order. However, as they are based on Newtonian mechanics, quantum effects important at low temperature are not properly characterized by AIMD, and, consequently, the application of AIMD is limited to temperatures above Debye temperature. The quantum behavior can be incorporated to AIMD making use of quantum thermal baths^{31,32}. However, this approach is exclusively valid for harmonic potentials^{33,34}. The problem is overcome by path-integral molecular dynamics (PIMD)³⁵, but the great computational cost of the method makes it challenging for density-functional theory (DFT) state-of-the-art calculations.

Aiming to overcome these difficulties, several methods have been developed recently to deal with anharmonic effects beyond perturbation theory^{12,36–41} mainly inspired by the self-consistent harmonic approximation (SCHA) devised by Hooton¹⁰. The main idea of the SCHA is that the system can be approximated by the harmonic potential that minimizes the free energy of the system, which does not necessarily coincide with the potential obtained from the second derivatives of the BO energy surface. The self-consistent *ab initio* lattice dynamics (SCAILD) method^{36,37} is an iterative way of converging the phonon frequencies at different temperatures accounting for anharmonic effects, but it does not optimize the eigenvectors of the harmonic potential nor the internal parameters in the crystal or molecular structure, and does not include anharmonic corrections in the free energy. The method presented by Antolin *et al.* does not include such corrections either³⁸. The temperature dependent effective potential (TDEP) technique can optimize the potential with respect to both polarization vectors and internal parameters, and, in principle, can include anharmonic corrections to the free energy through thermodynamic integration^{39,40}. Nevertheless, as it is based on AIMD calculations, it might break down below Debye temperature and the thermodynamic integration technique might be inefficient in their scheme⁴⁰. Finally, Monserrat *et al.* have recently presented a method in which the BO energy surface is Taylor expanded as a function of the harmonic normal coordinates⁴¹. The obtained Hamiltonian is solved variationally. In this scheme, the internal parameters of the crystal structure are not optimized, and the required mapping of the BO energy surface might demand a large computational effort.

In this paper we present a new implementation of the SCHA that is fully variational in the free energy. The free energy is explicitly minimized using a conjugate-gradient (CG) algorithm with respect to all the independent coefficients in a trial harmonic potential. Therefore, the method allows to access directly the anharmonic free en-

ergy of the system and optimizes the free energy with respect to phonon or vibron frequencies, polarization vectors and free parameters in the crystal or molecular structure. The temperature dependence is naturally incorporated into the formalism and temperature-dependent phonon dispersions or vibron frequencies can be readily calculated. The method is based on a stochastic evaluation of the free energy and its gradient. Thus, the cumbersome evaluation of anharmonic forces^{12,42} or mapping the BO energy surface is avoided. The method is named as the stochastic self-consistent harmonic approximation (SSCHA). It is perfectly valid to study both lattice or molecular vibrations, but, in order to simplify the text, we will use the language of crystals throughout. The SSCHA requires the calculation of total energies and forces on supercells with suitably chosen ionic configurations, which can be computed at any degree of theory. The SSCHA algorithm is devised to minimize the number of total energy and force calculations.

We apply the method to the strongly anharmonic platinum and palladium hydrides. In both cases the anharmonic correction to the phonon frequencies is larger than the harmonic frequencies themselves, invalidating any perturbative approach. We first study the role of anharmonicity in PtH at high pressure fully from first-principles, demonstrating that the high superconducting critical temperatures predicted in previous works^{43–45} are strongly suppressed by anharmonic effects. This result questions the interpretation suggested by several authors^{43–45} of the experiment in silane by Eremets *et al.*⁴⁶, where superconductivity was measured for the first time in a high-pressure hydride, stating that the measured superconductivity corresponded not to silane but to PtH. In palladium hydrides we show how within the SSCHA we can calculate thermodynamic properties in agreement with experiments in cases where the quasi-harmonic approximation breaks down.

The paper is structured as follows. In Sec. II we present the theoretical foundation of the SCHA and in Sec. III the way we implement it in a stochastic manner. In Secs. IV and V we apply the SSCHA to the strongly anharmonic platinum and palladium hydrides, where no perturbative approach is feasible. Finally, summary and conclusions are given in Sec. VI.

II. THE SELF-CONSISTENT HARMONIC APPROXIMATION

The SSCHA method applies to molecules and solids. In terms of notation clarity we treat the physical system as an isolated molecule throughout the manuscript. This means that in the case of periodic crystals we take a periodic supercell and treat the system at the Γ point. As it will be explained in Sec. IID, in the latter case we take advantage of translational symmetries.

Within the BO or adiabatic approximation, which assumes that the electrons adapt instantaneously to the

ionic positions, the dynamics of the ions in the supercell are determined by V , the potential defined by the BO energy surface. Normally, this potential is Taylor expanded as a function of the ionic displacements as

$$V = V_0 + \sum_{n=2}^{\infty} V_n, \quad (1)$$

where

$$V_n = \frac{1}{n!} \sum_{s_1 \dots s_n} \sum_{\alpha_1 \dots \alpha_n} \phi_{s_1 \dots s_n}^{\alpha_1 \dots \alpha_n} u^{s_1 \alpha_1} \dots u^{s_n \alpha_n} \quad (2)$$

and

$$u^{s\alpha} = R^{s\alpha} - R_{\text{eq}}^{s\alpha} \quad (3)$$

is the out-of-equilibrium displacement of atom s in the supercell along Cartesian coordinate α , with $R^{s\alpha}$ the corresponding atomic position and $R_{\text{eq}}^{s\alpha}$ the atomic equilibrium position. In Eq. (2) $\phi_{s_1 \dots s_n}^{\alpha_1 \dots \alpha_n}$ represents the n -th order derivative of the BO energy surface with respect to the atomic displacements calculated at equilibrium:

$$\phi_{s_1 \dots s_n}^{\alpha_1 \dots \alpha_n} = \left[\frac{\partial^{(n)} V}{\partial u^{s_1 \alpha_1} \dots \partial u^{s_n \alpha_n}} \right]_0. \quad (4)$$

Note that in Eq. (1) the first order term in the expansion vanishes as forces are zero at the equilibrium position.

Once the potential is defined, the dynamics of the ionic degrees of freedom are determined by the

$$H = T + V \quad (5)$$

Hamiltonian, where

$$T = \sum_{s=1}^N \sum_{\alpha=1}^3 \frac{(P^{s\alpha})^2}{2M_s} \quad (6)$$

is the kinetic-energy operator of the ions, with N the total number of atoms in the supercell, $P^{s\alpha}$ the momentum operator of the s -th atom along α , and M_s the mass of the s -th atom.

A. Formal definition of the self-consistent harmonic approximation

The free energy of the ionic Hamiltonian is given by the sum of the total energy and the entropic contribution:

$$F_H = \text{tr}[\rho_H H] + \frac{1}{\beta} \text{tr}[\rho_H \ln \rho_H] = -\frac{1}{\beta} \ln Z_H, \quad (7)$$

where the partition function is $Z_H = \text{tr}[e^{-\beta H}]$, the density matrix $\rho_H = e^{-\beta H}/Z_H$, and $\beta = 1/(k_B T)$. Calculating F_H represents a complicated task due to the many-body character of V . Instead, a quantum variational principle in the free energy can be defined substituting

the density matrix by any density matrix $\rho_{\mathcal{H}}$ defined by a trial $\mathcal{H} = T + \mathcal{V}$ Hamiltonian. Then, if

$$\mathcal{F}_H[\mathcal{H}] = \text{tr}[\rho_{\mathcal{H}} H] + \frac{1}{\beta} \text{tr}[\rho_{\mathcal{H}} \ln \rho_{\mathcal{H}}] \quad (8)$$

we have the so-called Gibbs-Bogoliubov inequality⁴⁷, namely

$$F_H \leq \mathcal{F}_H[\mathcal{H}]. \quad (9)$$

Adding and subtracting $\text{tr}[\rho_{\mathcal{H}} \mathcal{H}]$ in Eq. (8), it is straightforward to demonstrate that

$$\mathcal{F}_H[\mathcal{H}] = F_{\mathcal{H}} + \text{tr}[\rho_{\mathcal{H}} (V - \mathcal{V})]. \quad (10)$$

Obviously, the equality holds in Eq. (9) when $H = \mathcal{H}$. Thus, if $\mathcal{F}_H[\mathcal{H}]$ is minimized with respect to the trial \mathcal{H} Hamiltonian, a quantum variational principle is established valid at any temperature for the ionic problem.

The SCHA, which was originally proposed by Hooton¹⁰ and it was further developed by Choquard⁴⁸ and Werthamer⁴⁹, is obtained by restricting the trial potential \mathcal{V} to a harmonic one. The SCHA is analogous to the Hartree-Fock approximation for electrons in the sense that it assumes a trial density matrix formed by single-particle wave functions. As we shall see in Sec. II B, one advantage of taking a harmonic potential is that $F_{\mathcal{H}}$ and the probability density to find the system in a general \mathbf{R} ionic configuration, $\rho_{\mathcal{H}}(\mathbf{R}) = \langle \mathbf{R} | \rho_{\mathcal{H}} | \mathbf{R} \rangle$, can be expressed in a closed form in terms of phonon frequencies, polarization vectors and equilibrium positions.

The variational principle proposed by the SCHA allows us to treat systems beyond perturbation theory since, even if $V - V_2$ is large compared to V_2 itself invalidating any perturbative approach⁵⁻⁹, the variational principle is still valid. It should be remarked that in systems with huge anharmonicity phonons remain well-defined quasiparticles that are actually measured¹²⁻²⁹. Similarly, electrons in solids are existing quasiparticles despite being strongly affected by the electron-electron Coulomb interaction. Therefore, once the harmonic potential \mathcal{V} that minimizes $\mathcal{F}_H[\mathcal{H}]$ has been found, the eigenvalues of \mathcal{V} can be ascribed to the phonon spectra renormalized by anharmonic effects.

B. The harmonic Hamiltonian

The trial harmonic Hamiltonian of the SCHA is written in its general

$$\mathcal{H} = \sum_{s=1}^N \sum_{\alpha=1}^3 \frac{(P^{s\alpha})^2}{2M_s} + \frac{1}{2} \sum_{st} \sum_{\alpha\beta} u^{s\alpha} \Phi_{st}^{\alpha\beta} u^{t\beta} \quad (11)$$

form. The trial force-constants matrix $\Phi_{st}^{\alpha\beta}$ is different from the force-constants matrix associated to V_2 , $\phi_{st}^{\alpha\beta}$. Diagonalizing the dynamical matrix $\Phi_{st}^{\alpha\beta}/\sqrt{M_s M_t}$ as

$$\sum_{t=1}^N \sum_{\beta=1}^3 \frac{\Phi_{st}^{\alpha\beta}}{\sqrt{M_s M_t}} \epsilon_{\mu\mathcal{H}}^{t\beta} = \omega_{\mu\mathcal{H}}^2 \epsilon_{\mu\mathcal{H}}^{s\alpha}, \quad (12)$$

the polarization vectors $\epsilon_{\mu\mathcal{H}}^{s\alpha}$ and the $\omega_{\mu\mathcal{H}}$ phonon frequencies are obtained. These allow us to define the q_μ and p_μ normal coordinates that transform as

$$u^{s\alpha} = \sum_{\mu=1}^{3N} \frac{1}{\sqrt{M_s}} \epsilon_{\mu\mathcal{H}}^{s\alpha} q_\mu \quad (13)$$

$$P^{s\alpha} = \sum_{\mu=1}^{3N} \sqrt{M_s} \epsilon_{\mu\mathcal{H}}^{s\alpha} p_\mu. \quad (14)$$

Applying the change of variables in Eqs. (13) and (14) to Eq. (11), \mathcal{H} can be written as a sum of $3N$ independent oscillators:

$$\mathcal{H} = \sum_{\mu=1}^{3N} \left(\frac{p_\mu^2}{2} + \frac{\omega_{\mu\mathcal{H}}^2 q_\mu^2}{2} \right). \quad (15)$$

In Eqs. (12)-(15) μ is a mode index and the subindex \mathcal{H} in the phonon frequencies and polarization vectors denotes that they are associated to the harmonic Hamiltonian \mathcal{H} .

Once \mathcal{H} has been written as a sum of $3N$ independent harmonic oscillators, it is easy to observe that the probability to find the system in a general ionic configuration \mathbf{R} is (see Appendix A)

$$\rho_{\mathcal{H}}(\mathbf{R}) = A_{\mathcal{H}} \exp \left[- \sum_{st\alpha\beta\mu} \frac{\sqrt{M_s M_t}}{2a_{\mu\mathcal{H}}^2} \epsilon_{\mu\mathcal{H}}^{s\alpha} \epsilon_{\mu\mathcal{H}}^{t\beta} u^{s\alpha} u^{t\beta} \right], \quad (16)$$

where $A_{\mathcal{H}}$ is the normalization constant and

$$a_{\mu\mathcal{H}} = \sqrt{\hbar \coth(\beta \hbar \omega_{\mu\mathcal{H}}/2) / (2\omega_{\mu\mathcal{H}})} \quad (17)$$

is called the normal length of mode μ , even if it has units of length times square root of mass. Then, the quantum statistical average of any observable O that is exclusively a function of the atomic positions can be computed as

$$\text{tr}[\rho_{\mathcal{H}} O] = \int d\mathbf{R} O(\mathbf{R}) \rho_{\mathcal{H}}(\mathbf{R}). \quad (18)$$

Moreover, for a harmonic Hamiltonian its free energy can be calculated analytically from the well-known

$$F_{\mathcal{H}} = \sum_{\mu=1}^{3N} \left[\frac{1}{2} \hbar \omega_{\mu\mathcal{H}} - \frac{1}{\beta} \ln[1 + n_B(\omega_{\mu\mathcal{H}})] \right] \quad (19)$$

equation, where $n_B(\omega) = 1/(e^{\beta \hbar \omega} - 1)$ is the bosonic occupation factor. The fact that $F_{\mathcal{H}}$ and $\rho_{\mathcal{H}}(\mathbf{R})$ have the analytic forms given in Eqs. (16) and (19) will allow us to calculate easily the gradient of $\mathcal{F}_H[\mathcal{H}]$. Let us note that from Eqs. (10) and (18) we observe that the free energy can be calculated simply as

$$\mathcal{F}_H[\mathcal{H}] = F_{\mathcal{H}} + \int d\mathbf{R} [V(\mathbf{R}) - \mathcal{V}(\mathbf{R})] \rho_{\mathcal{H}}(\mathbf{R}), \quad (20)$$

where $V(\mathbf{R})$ is the BO energy of ionic configuration \mathbf{R} and $\mathcal{V}(\mathbf{R})$ is the trial harmonic energy for the same configuration.

C. The gradient of the free energy

Minimizing the free energy with respect to the trial harmonic Hamiltonian through a CG algorithm requires the knowledge of the gradient of the free energy with respect to all the parameters in \mathcal{H} . The trial \mathcal{H} contains two group of parameters: the \mathbf{R}_{eq} equilibrium positions and the $\Phi_{st}^{\alpha\beta}$ force-constants matrix. Thus, the gradient of the free energy can be written as $\nabla \mathcal{F}_H[\mathcal{H}] = (\nabla_{\mathbf{R}_{\text{eq}}} \mathcal{F}_H[\mathcal{H}], \nabla_{\Phi} \mathcal{F}_H[\mathcal{H}])$, where $\nabla_{\mathbf{R}_{\text{eq}}} \mathcal{F}_H[\mathcal{H}]$ is the gradient of the free energy with respect to the equilibrium positions and $\nabla_{\Phi} \mathcal{F}_H[\mathcal{H}]$ the gradient with respect to the force-constants matrix.

First of all, it can be shown that

$$\nabla_{\mathbf{R}_{\text{eq}}} \mathcal{F}_H[\mathcal{H}] = - \int d\mathbf{R} [\mathbf{f}(\mathbf{R}) - \mathbf{f}_{\mathcal{H}}(\mathbf{R})] \rho_{\mathcal{H}}(\mathbf{R}), \quad (21)$$

where $\mathbf{f}(\mathbf{R})$ is the vector formed by all the atomic forces for the ionic configuration \mathbf{R} and $\mathbf{f}_{\mathcal{H}}(\mathbf{R})$ denotes the vector formed by the forces derived from \mathcal{V} . Note that the integral with respect to the harmonic forces $\mathbf{f}_{\mathcal{H}}(\mathbf{R})$ vanishes, but, as we shall explain below, it is convenient to write the integral in this form. On the other hand, the gradient with respect to the force-constants matrix is given by

$$\begin{aligned} \nabla_{\Phi} \mathcal{F}_H[\mathcal{H}] = & - \sum_{st\alpha\beta\mu} \sqrt{\frac{M_t}{M_s}} (\epsilon_{\mu\mathcal{H}}^{s\alpha} \nabla_{\Phi} \ln a_{\mu\mathcal{H}} + \nabla_{\Phi} \epsilon_{\mu\mathcal{H}}^{s\alpha}) \epsilon_{\mu\mathcal{H}}^{t\beta} \\ & \times \int d\mathbf{R} [f^{s\alpha}(\mathbf{R}) - f_{\mathcal{H}}^{s\alpha}(\mathbf{R})] (R^{t\beta} - R_{\text{eq}}^{t\beta}) \rho_{\mathcal{H}}(\mathbf{R}). \end{aligned} \quad (22)$$

The procedure to derive Eqs. (21) and (22) is sketched in Appendix A. Let us note that both $\nabla_{\Phi} a_{\mu\mathcal{H}}$ and $\nabla_{\Phi} \epsilon_{\mu\mathcal{H}}^{s\alpha}$ are analytic functions of phonon frequencies and polarizations as shown in Appendix A.

The CG minimization is started from a trial initial harmonic Hamiltonian \mathcal{H}_0 , which is defined following Eqs. (3) and (11) from the $\mathbf{R}_{\text{eq}0}$ starting equilibrium positions and the starting $\Phi(0)$ force-constants matrix. After calculating the gradient as explained in Eqs. (21) and (22), the first CG step allows us to update the equilibrium positions and the force-constants matrix to $\mathbf{R}_{\text{eq}1}$ and $\Phi(1)$, from which we obtain the \mathcal{H}_1 Hamiltonian corresponding to first CG step. Similarly, at each j CG step of the minimization the equilibrium positions and the force-constants matrix are updated to $\mathbf{R}_{\text{eq}j}$ and $\Phi(j)$, which define the Hamiltonian at step j , \mathcal{H}_j . The minimization should be carried on until the gradient vanishes.

D. Symmetries and the independent coefficients in the trial \mathcal{H}

We consider that the anharmonic Hamiltonian given by the SSCHA has the same symmetries as the harmonic Hamiltonian. Therefore, at any CG step j the Hamiltonian \mathcal{H}_j will respect the symmetries of the harmonic

Hamiltonian. Considering that \mathcal{H}_j is determined by the $\Phi(j)$ force-constants matrix and the $\mathbf{R}_{\text{eq}j}$ equilibrium positions, the symmetries of the Hamiltonian are determined by the symmetries of both $\mathbf{R}_{\text{eq}j}$ and $\Phi(j)$. In the SSCHA we consider translational, time-reversal and crystal symmetries to determine the independent coefficients in the equilibrium positions and the force-constants matrix.

If symmetries were neglected, throughout the minimization the equilibrium positions could change in any direction within the unit cell. All these possible displacements can be described with $3n$ size real vectors that form a vector space of dimension $3n$, where n is the number of atoms in the unit cell. The scalar product in this vector space is defined as

$$\langle \chi, \xi \rangle = \sum_{\bar{s}\alpha} \chi^{\bar{s}\alpha} \xi^{\bar{s}\alpha}, \quad (23)$$

where χ and ξ are elements of the vector space. Let $\{\chi_{(\text{ns})}(l)\}_{l=1,\dots,3n}$ be an orthonormal basis of this vector space. Then, the vectors of the basis satisfy the

$$\langle \chi_{(\text{ns})}(l), \chi_{(\text{ns})}(l') \rangle = \delta_{ll'} \quad (24)$$

orthonormality condition. The bar in the atom index \bar{s} in Eq. (23) denotes that it is an atom of the unit cell and the (ns) subscript that the basis vectors have not been symmetrized. Thus, the equilibrium positions at a CG iteration j could be given as

$$R_{\text{eq}j}^{\bar{s}\alpha} = R_{\text{eq}0}^{\bar{s}\alpha} + \sum_{l=1}^{3n} \kappa_{j(\text{ns})}(l) \chi_{(\text{ns})}^{\bar{s}\alpha}(l), \quad (25)$$

where the $\kappa_{j(\text{ns})}(l)$ coefficients would determine how much the atoms would be displaced along $\chi_{(\text{ns})}(l)$ at iteration j . Obviously, $\kappa_{0(\text{ns})}(l) = 0$. In the SSCHA however we allow the equilibrium positions to change exclusively in the subspace of this vector space that respects crystal symmetries.

In order to obtain a basis of the symmetrized subspace we need to take into account all the $\hat{S} \equiv \{S, \mathbf{v}\}$ symmetry operations of the space group of the crystal. Here, S is a 3×3 orthogonal matrix and \mathbf{v} is the vector defining the fractional translation of the crystal operation \hat{S} . The S matrices form the point group of the crystal. We symmetrize the $\{\chi_{(\text{ns})}(l)\}_{l=1,\dots,3n}$ basis vectors applying all the symmetry operations \hat{S} as⁵⁰

$$\chi_{(\bar{s})}^{\bar{s}\alpha}(l) = \frac{1}{N_S} \sum_{\hat{S}} \sum_{\beta} S^{\alpha\beta} \chi_{(\text{ns})}^{\hat{S}^{-1}(\bar{s})\beta}(l), \quad (26)$$

where \hat{S}^{-1} is the inverse symmetry operation of \hat{S} . The sum in Eq. (26) runs over all the N_S symmetry operations and $\hat{S}^{-1}(\bar{s})$ labels the atom into which the \bar{s} -th atom transforms after the application of \hat{S}^{-1} modulo a lattice translation vector. The (s) subscript denotes that the vectors respect symmetries. Note that

Eq. (26) is commonly used in DFT codes to symmetrize the forces on the atoms, and when the electronic \mathbf{k} -point mesh is reduced by symmetry. When we symmetrize the basis vectors as shown in Eq. (26), many of these $\chi_{(\bar{s})}(l)$ vectors become linearly dependent. We pick exclusively the linearly independent vectors applying a Gram-Schmidt orthonormalization procedure. The basis vectors of the symmetrized subspace are labeled as $\{\chi(l)\}_{l=1,\dots,n_w}$, where n_w is the number of linearly independent basis vectors after the symmetrization. The Gram-Schmidt orthonormalization guarantees that the $\chi(l)$ vectors satisfy Eq. (24). The value of n_w must be equal to the number of free internal parameters in the Wyckoff positions of the crystal structure.

Once we have determined the symmetry reduced basis, at a given iteration j in the CG minimization the equilibrium position of the atoms can be described as

$$R_{\text{eq}j}^{\bar{s}\alpha} = R_{\text{eq}0}^{\bar{s}\alpha} + \sum_{l=1}^{n_w} \kappa_j(l) \chi^{\bar{s}\alpha}(l), \quad (27)$$

where the $\kappa_j(l)$ coefficient determines how much the atoms are displaced along the symmetrized $\chi(l)$ direction at iteration j . Then, it is easy to relate $\nabla_{\mathbf{R}_{\text{eq}}} \mathcal{F}_H[\mathcal{H}_j]$ with the derivatives of the free energy with respect to the $\kappa_j(l)$ coefficients introduced in Eq. (27):

$$\frac{\partial \mathcal{F}_H[\mathcal{H}_j]}{\partial \kappa_j(l)} = \sum_{s\alpha} \chi^{s\alpha}(l) \frac{\partial \mathcal{F}_H[\mathcal{H}_j]}{\partial R_{\text{eq}j}^{s\alpha}}, \quad (28)$$

where $\frac{\partial \mathcal{F}_H[\mathcal{H}_j]}{\partial R_{\text{eq}j}^{s\alpha}}$ is given in Eq. (21).

In order to determine how Φ can change in the SSCHA minimization respecting crystal, time-reversal and translational symmetries, we proceed in an analogous way. In general Φ is a matrix that belongs to the group of $3N \times 3N$ Hermitian matrices. The Hermitian matrices form a vector space and the scalar product between two elements of the vector space is defined as

$$\langle \mathcal{G}, \mathcal{T} \rangle = \sum_{st\alpha\beta} \mathcal{G}_{st}^{\alpha\beta} \mathcal{T}_{st}^{\alpha\beta*}, \quad (29)$$

where \mathcal{G} and \mathcal{T} are two elements of the vector space. We start with the subspace of this vector space that preserves translational symmetries but has not been symmetrized with the \hat{S} crystal symmetry operations nor time-reversal. Let $\{\mathcal{G}_{(\text{ns})}(m)\}_{m=1,\dots,(3n)^2 N_1 N_2 N_3}$ be an orthonormal basis of this vector space so that

$$\langle \mathcal{G}_{(\text{ns})}(m), \mathcal{G}_{(\text{ns})}(m') \rangle = \delta_{mm'}. \quad (30)$$

Thanks to Bloch's theorem, the dimension of this vector space is $(3n)^2 \times N_1 \times N_2 \times N_3$, where $N_1 \times N_2 \times N_3$ is the supercell size. As any matrix belonging to this vector space respects translational symmetries, the Fourier transform of a matrix described in the $\{\mathcal{G}_{(\text{ns})}(m)\}_{m=1,\dots,(3n)^2 N_1 N_2 N_3}$ basis is block-diagonal and can be defined with a single \mathbf{q} vector in the first Brillouin zone (1BZ). Thus, if only

transitional symmetries were considered, the evolution of the force-constants matrix in the minimization could be described as

$$\Phi(j) = \sum_{m=1}^{(3n)^2 N_1 N_2 N_3} c_{j(\text{ns})}(m) \mathcal{G}_{(\text{ns})}(m), \quad (31)$$

where the $c_{j(\text{ns})}(m)$ coefficients would determine the value of the force-constants matrix at CG step j . Nevertheless, in the SSCHA we allow the force-constants matrix to vary exclusively in the subspace of this vector space that respects the \hat{S} crystal symmetries⁵¹ and time-reversal symmetry.

The elements of the basis are symmetrized according to the \hat{S} symmetry operations and time-reversal as shown in Appendix B. After the symmetrization, the basis is reduced making use of a Gram-Schmidt orthonormalization procedure so that only the linearly independent elements of the symmetrized basis are considered. This process yields a new $\{\mathcal{G}(m)\}_{m=1, \dots, N_R}$ basis that respects translational, crystal and time-reversal symmetries. N_R is the dimension of the fully symmetrized subspace. We construct the force-constants matrix as

$$\Phi(j) = \sum_{m=1}^{N_R} c_j(m) \mathcal{G}_{st}^{\alpha\beta}(m). \quad (32)$$

The $c_j(m)$ coefficients unambiguously determine the force-constants matrix at each CG iteration j . With the $\mathcal{G}(m)$ matrices it is easy to relate the derivative of the free energy with respect to the $c_j(m)$ coefficients with $\nabla_{\Phi} \mathcal{F}_H[\mathcal{H}_j]$. From Eq. (32) straightforwardly

$$\frac{\partial \mathcal{F}_H[\mathcal{H}_j]}{\partial c_j(m)} = \sum_{st\alpha\beta} \mathcal{G}_{st}^{\alpha\beta}(m) \frac{\partial \mathcal{F}_H[\mathcal{H}_j]}{\partial \Phi_{st}^{\alpha\beta}(j)}, \quad (33)$$

where the $\frac{\partial \mathcal{F}_H[\mathcal{H}_j]}{\partial \Phi_{st}^{\alpha\beta}(j)}$ derivatives are given in Eq. (22).

In order to illustrate the reduction of coefficients, let us consider a $4 \times 4 \times 4$ supercell of a rock-salt structure. In this case, the *a priori* 2304 $c_{(\text{ns})}(m)$ free parameters in the force-constants matrix in Eq. (31) are reduced to simply 50 $c(m)$ parameters in Eq. (32).

Considering the independent coefficients that we have found after the symmetry analysis, we can write the gradient of the free energy as $\nabla \mathcal{F}_H[\mathcal{H}] = (\nabla_{\kappa} \mathcal{F}_H[\mathcal{H}], \nabla_c \mathcal{F}_H[\mathcal{H}])$. The number of components in this gradient is much fewer than the components in $(\nabla_{\mathbf{R}_{\text{eq}}} \mathcal{F}_H[\mathcal{H}], \nabla_{\Phi} \mathcal{F}_H[\mathcal{H}])$. Therefore, in the SSCHA we work with $\nabla \mathcal{F}_H[\mathcal{H}] = (\nabla_{\kappa} \mathcal{F}_H[\mathcal{H}], \nabla_c \mathcal{F}_H[\mathcal{H}])$. At a given iteration j of the CG minimization, the components of $\nabla_{\kappa} \mathcal{F}_H[\mathcal{H}_j]$ are given in Eq. (28) and the components of $\nabla_c \mathcal{F}_H[\mathcal{H}_j]$ in Eq. (33).

III. THE STOCHASTIC IMPLEMENTATION OF THE SELF-CONSISTENT HARMONIC APPROXIMATION

The calculation of the integrals in Eqs. (20)-(22) needed to get the free energy and its gradient is a complicated task⁵. In principle, it requires the calculation of high-order $\phi_{s_1 \dots s_n}^{\alpha_1 \dots \alpha_n}$ anharmonic coefficients that allow an accurate estimation of the \mathbf{f} forces and the V potential. Third order anharmonic coefficients can be calculated nowadays through first-principles calculations using the $2n + 1$ theorem⁹. However, one should note that third order terms do not contribute in Eq. (22). The reason is that the integrand is odd for third order terms and, thus, the integral vanishes by symmetry. Therefore, one needs to go at least to the fourth order to apply the SCHA. The calculation of the fourth order anharmonic coefficients is extremely cumbersome as it requires performing first order numerical derivatives of third order anharmonic terms or second order numerical derivatives of dynamical matrices calculated in supercells^{6,8,12,42,52,53}. Consequently, calculating fourth-order anharmonic coefficients remains a complicated computational problem and these coefficients have been calculated *ab initio* exclusively for some specific \mathbf{q} points in the 1BZ or in very simple crystal structures^{6,8,12,42,52,53}. Therefore, the SCHA has been applied calculating explicitly the fourth-order anharmonic coefficients in the whole 1BZ purely *ab initio* only in the high-pressure simple cubic phase of calcium^{12,42}. Moreover, the restriction to fourth-order terms is an approximation that could be inappropriate and should be verified case by case.

In the SSCHA we take a different approach and, instead of calculating $\phi_{i_1 \dots i_n}^{\alpha_1 \dots \alpha_n}$ coefficients, we evaluate the integrals stochastically using suitably chosen ionic configurations in supercells without assuming any Taylor development. The stochastic evaluation of the quantum statistical average of any observable is performed taking advantage of the analytic behavior of $\rho_{\mathcal{H}}(\mathbf{R})$ and making use of importance sampling and reweighting techniques.

A. Stochastic calculation of the gradient

As it was mentioned above, the minimization of $\mathcal{F}_H[\mathcal{H}]$ is started from an arbitrary harmonic Hamiltonian \mathcal{H}_0 . Then, we create a set of $\{\mathbf{R}_I\}_{I=1, \dots, N_c}$ ionic configurations in the supercell according to the $\rho_{\mathcal{H}_0}(\mathbf{R})$ distribution given in Eq. (16). The distribution is determined by the starting $\mathbf{R}_{\text{eq}0}$ equilibrium positions and the starting $\Phi(0)$ force-constants matrix, and can be created using random numbers generated with a pure Gaussian distribution as shown in Appendix C. According to the importance sampling technique, any quantum statistical average of an operator that exclusively depends on the atomic positions can be evaluated as an average of the operator

over the created N_c configurations. Namely,

$$\int d\mathbf{R} O(\mathbf{R}) \rho_{\mathcal{H}_0}(\mathbf{R}) \simeq \frac{1}{N_c} \sum_{I=1}^{N_c} O(\mathbf{R}_I) \equiv \langle O \rangle, \quad (34)$$

where $O(\mathbf{R}_I)$ denotes the value of the operator $O(\mathbf{R})$ at the configuration \mathbf{R}_I . In Eq. (34) the equality holds when $N_c \rightarrow \infty$ and the error in the stochastic evaluation vanishes. Therefore, we evaluate BO energies and atomic forces in the $\{\mathbf{R}_I\}_{I=1,\dots,N_c}$ configurations, $V(\mathbf{R}_I)$ and $\mathbf{f}(\mathbf{R}_I)$, respectively, and calculate the integrals in Eqs. (20)-(22) following the stochastic procedure of Eq. (34). Once these are computed, $\nabla \mathcal{F}_H[\mathcal{H}_0]$ can be obtained stochastically and the first CG step can be performed to obtain \mathcal{H}_1 .

After the first CG step, the ionic configurations should in principle be regenerated as in Eq. (16) using the new trial Hamiltonian \mathcal{H}_1 , which is defined by the \mathbf{R}_{eq1} equilibrium positions and the $\Phi(1)$ force-constants matrix. Thus, in order to calculate the gradient we should recalculate BO energies and atomic forces in the supercell in the new set of configurations defined by $\rho_{\mathcal{H}_1}(\mathbf{R})$. Considering that in general hundreds of CG steps are needed to find the minimum of the free energy, calculating BO energies and forces from first-principles at each CG step would make the method prohibitively time-demanding. We adopt a reweighting procedure to avoid this issue and use the BO energies and atomic forces of the initial $\{\mathbf{R}_I\}_{I=1,\dots,N_c}$ set throughout the CG minimization. At step j of the CG minimization, this is achieved including the $\rho_{\mathcal{H}_j}(\mathbf{R})/\rho_{\mathcal{H}_0}(\mathbf{R})$ factor in the importance sampling evaluation of the integrals. Note that in the first $j = 0$ step the factor is equal to one. Therefore, at step j of the

CG minimization the integral in Eq. (34) is computed as if the initial $\{\mathbf{R}_I\}_{I=1,\dots,N_c}$ set was generated according to $\rho_{\mathcal{H}_j}(\mathbf{R})$, namely

$$\int d\mathbf{R} O(\mathbf{R}) \rho_{\mathcal{H}_j}(\mathbf{R}) \simeq \frac{1}{N_c} \sum_{I=1}^{N_c} O(\mathbf{R}_I) \frac{\rho_{\mathcal{H}_j}(\mathbf{R}_I)}{\rho_{\mathcal{H}_0}(\mathbf{R}_I)} = \langle O \rho_{\mathcal{H}_j} / \rho_{\mathcal{H}_0} \rangle. \quad (35)$$

The stochastic error in Eq. (35) can be evaluated as

$$\Delta \langle O \rho_{\mathcal{H}_j} / \rho_{\mathcal{H}_0} \rangle = \frac{1}{\sqrt{N_c}} \sqrt{s_{O \rho_{\mathcal{H}_j} / \rho_{\mathcal{H}_0}}^2}, \quad (36)$$

where

$$s_P^2 = \frac{1}{N_c - 1} \sum_{I=1}^{N_c} [P(\mathbf{R}_I) - \langle P \rangle]^2 \quad (37)$$

is the variance of function $P(\mathbf{R})$ ⁵⁴. Following Eq. (35), the free energy in Eq. (20) and its gradient in Eqs. (21) and (22) are calculated at a given iteration j of the CG minimization simply as

$$\mathcal{F}_H[\mathcal{H}_j] \simeq F_{\mathcal{H}_j} + \frac{1}{N_c} \sum_{I=1}^{N_c} [V(\mathbf{R}_I) - \mathcal{V}_j(\mathbf{R}_I)] \frac{\rho_{\mathcal{H}_j}(\mathbf{R}_I)}{\rho_{\mathcal{H}_0}(\mathbf{R}_I)} \quad (38)$$

$$\nabla_{\mathbf{R}_{\text{eq}}} \mathcal{F}_H[\mathcal{H}_j] \simeq -\frac{1}{N_c} \sum_{I=1}^{N_c} [\mathbf{f}(\mathbf{R}_I) - \mathbf{f}_{\mathcal{H}_j}(\mathbf{R}_I)] \frac{\rho_{\mathcal{H}_j}(\mathbf{R}_I)}{\rho_{\mathcal{H}_0}(\mathbf{R}_I)} \quad (39)$$

$$\nabla_{\Phi} \mathcal{F}_H[\mathcal{H}_j] \simeq - \sum_{st\alpha\beta\mu} \sqrt{\frac{M_t}{M_s}} (\epsilon_{\mu\mathcal{H}_j}^{s\alpha} \nabla_{\Phi} \ln a_{\mu\mathcal{H}_j} + \nabla_{\Phi} \epsilon_{\mu\mathcal{H}_j}^{s\alpha}) \epsilon_{\mu\mathcal{H}_j}^{t\beta} \frac{1}{N_c} \sum_{I=1}^{N_c} [f^{s\alpha}(\mathbf{R}_I) - f_{\mathcal{H}_j}^{s\alpha}(\mathbf{R}_I)] (R_I^{t\beta} - R_{\text{eqj}}^{t\beta}) \frac{\rho_{\mathcal{H}_j}(\mathbf{R}_I)}{\rho_{\mathcal{H}_0}(\mathbf{R}_I)}. \quad (40)$$

In Eqs. (38)-(40) the equality holds when $N_c \rightarrow \infty$.

Let us note that, despite the contribution of $\mathbf{f}_{\mathcal{H}}$ in Eq. (39) vanishes and is analytic in Eq. (40) (see Appendix A), it is convenient to keep this contribution explicitly in the stochastic evaluation of the gradient. Similarly, in the stochastic evaluation of the free energy in Eq. (38), it is convenient to keep the \mathcal{V} contribution even if it is analytic as well. The reason is that in this way the stochastic analysis is performed exclusively on the anharmonic part of the forces or the BO energies, reducing the stochastic error. Therefore, at each step j of the CG minimization $\mathbf{f}_{\mathcal{H}_j}(\mathbf{R}_I)$ and $\mathcal{V}_j(\mathbf{R}_I)$ are calculated, which are analytic functions of the $\omega_{\mu\mathcal{H}_j}$ frequencies and $\epsilon_{\mu\mathcal{H}_j}^{s\alpha}$ polarizations. The fact that including $\mathbf{f}_{\mathcal{H}_j}(\mathbf{R}_I)$ and $\mathcal{V}_j(\mathbf{R}_I)$ in the evaluation of the free energy and its gradient is beneficial

for the stochastic approach is exemplified if we assume the $V(\mathbf{R})$ potential is perfectly harmonic and the initial \mathcal{H}_0 is the harmonic Hamiltonian. Then, the gradient obtained in the first step stochastically is exactly zero, with no stochastic error, as $\mathbf{f}(\mathbf{R}_I) - \mathbf{f}_{\mathcal{H}_0}(\mathbf{R}_I) = 0$. Similarly, the free energy would not have any stochastic error since $V(\mathbf{R}_I) - \mathcal{V}_0(\mathbf{R}_I) = 0$, and $\mathcal{F}_H[\mathcal{H}_0] = F_{\mathcal{H}_0}$. If $\mathbf{f}_{\mathcal{H}_0}(\mathbf{R}_I)$ and $\mathcal{V}_0(\mathbf{R}_I)$ were not included in the stochastic evaluation of the integrals by using their analytic expression instead, the stochastic error would not vanish.

As shown above, the free energy and its gradient can be obtained calculating BO energies and ionic forces on supercells with suitably chosen ionic configurations. The calculation of the BO energies and forces can be performed using a model or *ab initio* potentials. It is note-

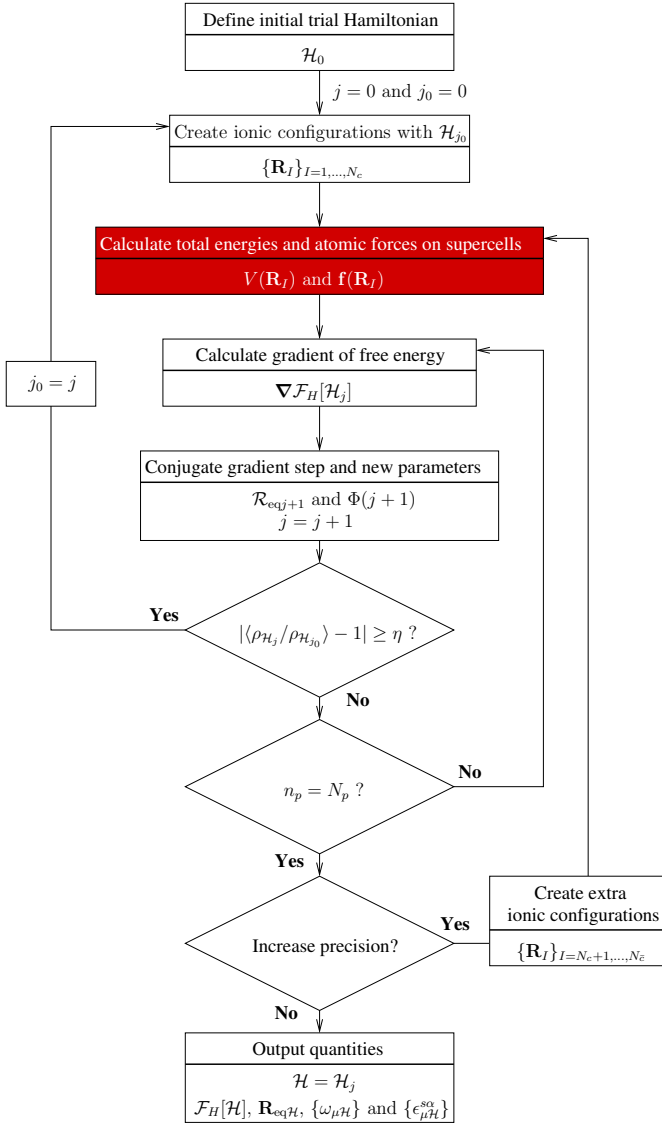


FIG. 1. (Color online) Schematic representation of the SSCHA calculation flowchart. See Sec. III B of the main text for the definition of the symbols. The step in the algorithm marked in red, the calculation of the total energies and forces on supercells, is performed with any external total-energy-force engine. In case an *ab initio* approach is taken, it represents all the computer time of the SSCHA minimization.

worthy that calculating the forces from first-principles requires a negligible additional effort in a total energy calculation because of the Hellmann-Feynman theorem^{55,56}. Hence, the way of minimizing the gradient sketched above is very convenient for applying the SSCHA fully from first-principles, specially, due to the reweighting procedure.

B. Stopping criteria and calculation flowchart

In principle, the minimization should continue till all the components of the gradient are smaller than a given threshold value. The threshold value should be chosen so that phonon frequencies and equilibrium positions are converged with respect to it. When all components of the gradient are smaller than the threshold value the minimum of the free energy has been found and \mathcal{H}_j is the harmonic Hamiltonian that minimizes it, j being the final step. Then, the $\mathbf{R}_{\text{eq},j}$ are the final equilibrium atomic positions, $\{\omega_{\mu\mathcal{H}_j}\}$ form the SSCHA phonon spectra and $\{\epsilon_{\mu\mathcal{H}_j}^{s\alpha}\}$ are the final polarization vectors, which are obtained diagonalizing the $\Phi(j)$ force-constants matrix, and $\mathcal{F}_H[\mathcal{H}_j]$ is the final vibrational free energy.

Considering that $\nabla_{\kappa}\mathcal{F}_H[\mathcal{H}_j]$ and $\nabla_c\mathcal{F}_H[\mathcal{H}_j]$ have different units, we should use different threshold values for each of them, let's say ζ_{κ} and ζ_c , respectively. Thus, if

$$|\nabla_h^i\mathcal{F}_H[\mathcal{H}_j]| < \zeta_h, \quad (41)$$

where h denotes κ or c and $\nabla_h^i\mathcal{F}_H[\mathcal{H}_j]$ is the i -th component of the gradient at CG step j , the i -th parameter is not updated in the $j+1$ step.

Due to the stochastic origin of the method, we can account for the error of the gradient as shown in Eq. (36) in the minimization and devise a second stopping criteria. We define a meaningfulness parameter θ and in case

$$\theta\Delta(\nabla^i\mathcal{F}_H[\mathcal{H}_j]) > |\nabla^i\mathcal{F}_H[\mathcal{H}_j]|, \quad (42)$$

where $\Delta(\nabla^i\mathcal{F}_H[\mathcal{H}_j])$ is the stochastic error of the i -th component of the gradient, the i -th parameter is not updated in the $j+1$ step. From now on, let n_p be the number of components of the gradient satisfying Eq. (41) or (42), and N_p the total number of components of the gradient.

Moreover, if $\langle\rho_{\mathcal{H}_j}/\rho_{\mathcal{H}_0}\rangle$ deviates significantly from 1 the gradient cannot be stochastically evaluated accurately because the initial set of configurations does not represent closely the $\rho_{\mathcal{H}_j}(\mathbf{R})$ distribution. Hence, if

$$|\langle\rho_{\mathcal{H}_j}/\rho_{\mathcal{H}_0}\rangle - 1| \geq \eta, \quad (43)$$

where η is a small positive number, generally between 0.2 and 0.3, we consider that the stochastic evaluation of the gradient is poor and the minimization is stopped at the CG step j .

The SSCHA calculation flowchart is sketched in Fig. 1. As mentioned above, the minimization is stopped at step j if (i) $n_p = N_p$ or (ii) the stochastic evaluation is poor according to Eq. (43). If condition (ii) is satisfied at CG step j , the $\rho_{\mathcal{H}_j}(\mathbf{R})$ probability distribution is used to create a new set of $\{\mathbf{R}_I\}_{I=1,...,N_c}$ configurations for which total energies and atomic forces are recomputed. Then, the minimization continues using this new set of configurations. On the other hand, if condition (i) is fulfilled, one needs to see whether the stochastic accuracy

is satisfactory. If it is so, the calculation is finished and the minimum is found. If, on the contrary, one wants to increase the precision in the evaluation of the gradient, the number of configurations should be increased in order to reduce the error. This can be done generating $N_{\bar{e}} - N_c$ new configurations with the last Hamiltonian used to generate configurations in order to increase the size of the set to $N_{\bar{e}}$. Then, new total energies and atomic forces are calculated in the new $N_{\bar{e}} - N_c$ configurations and the process continues till the stochastic uncertainty is reduced up to a satisfactory level. This should be noted in the convergence of the phonon spectra.

The calculation of total energies and atomic forces needed in the SSCHA algorithm can be performed at any degree of theory with any external total-energy-force engine. If an *ab initio* approach is taken, practically all the computer time goes in the calculation of the total energies and forces. The algorithm sketched in Fig. 1 is devised to minimize the number of calls to the total-energy-force engine. For instance, one can start with a small number of N_c until the calculation stops because $n_p = N_p$. The size of the set can be increased at this point to gain accuracy. Thus, the number of calls to the total-energy-force engine can be effectively optimized in the SSCHA algorithm. Obviously, the number of total energy and atomic force calculations is reduced in case the starting \mathcal{H}_0 is close to the \mathcal{H} Hamiltonian that minimizes the free energy. This way, the need to redefine a new set of configurations might be avoided. Anyway, the final result is independent of the starting \mathcal{H}_0 .

C. Temperature dependence in the SSCHA

The temperature dependence in the SSCHA is naturally incorporated. As shown in Eqs. (20)-(22), the free energy and its gradient depend on temperature through the temperature dependence of $F_{\mathcal{H}}$ (see Eq. (19)) and $\rho_{\mathcal{H}}(\mathbf{R})$, which depends on temperature via the normal lengths $a_{\mu\mathcal{H}}$ (see Eqs. (16) and (17)). When creating the set of configurations $\{\mathbf{R}_I\}_{I=1,\dots,N_c}$ the temperature dependence is incorporated as the $a_{\mu\mathcal{H}}$ normal lengths are used to generate the set as noted in Appendix C. Thus, in principle, one should use a given set of configurations for each temperature, calculating new forces and BO energies for each temperature.

Nevertheless, a recycling scheme can be adopted to use the set of configurations created with a given temperature T_0 (and the forces and BO energies calculated for them) to perform the minimization at a different temperature T . In order to do so, in Eqs. (38)-(40) we modify the factor used in the reweighting as

$$\frac{\rho_{\mathcal{H}_j}(\mathbf{R}_I)}{\rho_{\mathcal{H}_0}(\mathbf{R}_I)} \rightarrow \frac{\rho_{\mathcal{H}_j}(\mathbf{R}_I, T)}{\rho_{\mathcal{H}_0}(\mathbf{R}_I, T_0)}, \quad (44)$$

where $\rho_{\mathcal{H}_0}(\mathbf{R}_I, T_0)$ is the probability distribution function used to generate the $\{\mathbf{R}_I\}_{I=1,\dots,N_c}$ configurations and $\rho_{\mathcal{H}_j}(\mathbf{R}_I, T)$ is the probability distribution at CG step

j for temperature T at which the free energy wants to be minimized. We should note that when adopting this recycling scheme at $j = 0$ $\langle \rho_{\mathcal{H}_0}(T) / \rho_{\mathcal{H}_0}(T_0) \rangle$ is different from one. Thus, we use the criteria defined in Eq. (43) to discern whether recycling the configurations created with a different temperature is valid.

IV. APPLICATION OF THE STOCHASTIC SELF-CONSISTENT HARMONIC APPROXIMATION TO PLATINUM HYDRIDE AT HIGH PRESSURE

Motivated by the quest for metallic and superconducting hydrogen at very high pressure⁵⁷, many first-principles calculations based on the harmonic approximation have been performed in the last years in compressed hydrides predicting high values for the superconducting critical temperature (T_c)^{43,58-62}. Nevertheless, the only experimental evidence so far of superconductivity in hydrides at high pressure was found in SiH₄ around 100 GPa with $T_c = 17$ K⁴⁶. However, it is not clear whether the superconductivity of SiH₄ was actually measured. Degtyareva *et al.* proposed that PtH could have been formed in that experiment if silane decomposed releasing hydrogen that reacted with the platinum electrodes⁶³. It has been argued^{45,63} that the formation of PtH might explain the x-ray diffraction pattern observed in Ref. 46, and that the observed superconductivity might be attributed to the superconductivity of PtH as its calculated T_c is not far from the measured value⁴³⁻⁴⁵. However, in PtH T_c has been calculated within the harmonic approximation and it is not clear whether anharmonicity might affect this result, as it does in the very similar PdH²⁵. We apply the SSCHA method to high-pressure PtH to shine light on this issue.

A. Calculation details

We apply the SSCHA in PtH at 100 GPa and 0 K. Even if at ambient conditions Pt and H are immiscible, at high pressure platinum hydride can be synthesized⁴⁴. Experimentally it was observed that above 42 GPa PtH adopts a hexagonal closed-packed (hcp) structure⁴⁴ and, consequently, we use the hcp phase in our calculations. We take the lattice parameters that minimize the electronic energy at 100 GPa, namely $a = 5.1203$ a.u. and $c = 8.6471$ a.u. The SSCHA is applied fully *ab initio* with forces and BO energies calculated using DFT within the Perdew-Burke-Ernzerhof generalized gradient approximation⁶⁴ and using ultrasoft pseudopotentials as implemented in QUANTUM-ESPRESSO⁵⁰. A 60 Ry energy cutoff is used and a $26 \times 26 \times 16$ mesh for the 1BZ integrations in the unit cell. Phonon frequencies and deformation potentials are calculated within linear response^{2,50} in a $6 \times 6 \times 4$ \mathbf{q} point grid. For the SSCHA a $2 \times 2 \times 1$ supercell containing 16 atoms is chosen. Af-

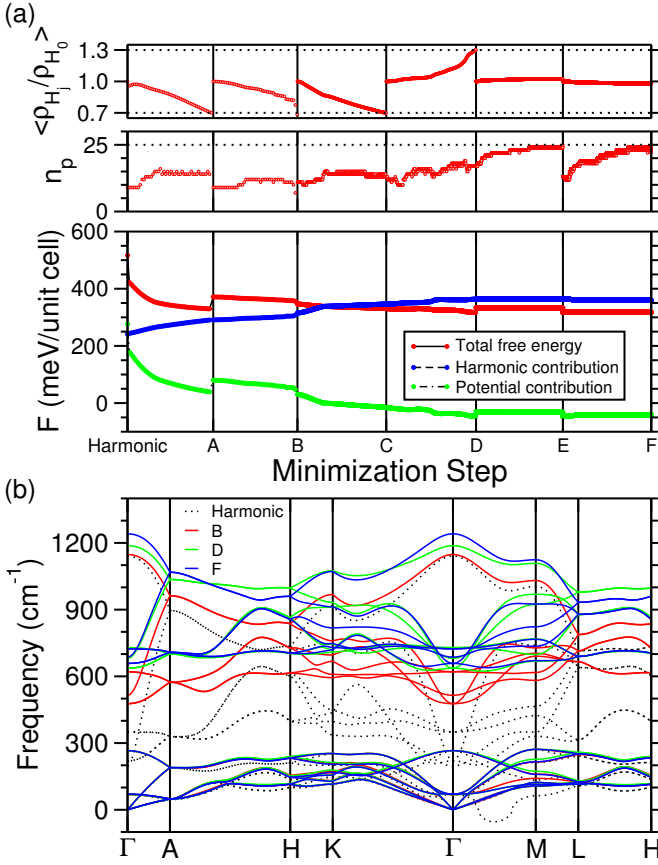


FIG. 2. (Color online) The evolution of the SSCHA calculation in PtH at 0 K and 100 GPa. The starting Hamiltonian is the harmonic one. The parameters of the calculation are $\theta = 1$, $\zeta_c = 0.0003$ a.u.² and $\eta = 0.3$ (see Sec. IV A). In (a) we depict the evolution of $\langle \rho_{\mathcal{H}_j} / \rho_{\mathcal{H}_0} \rangle$, n_p , the number of parameters that are not updated according to Eqs. (41) or (42), and the free energy throughout the minimization. In this calculation the total number of parameters in the gradient is $N_p = 25$. In these figures each point represents a CG step. The total vibrational free energy $\mathcal{F}_H[\mathcal{H}_j] = F_{\mathcal{H}_j} + \text{tr}[\rho_{\mathcal{H}_j}(V - \mathcal{V}_j)]$, the harmonic contribution $F_{\mathcal{H}_j}$, and the potential contribution $\text{tr}[\rho_{\mathcal{H}_j}(V - \mathcal{V}_j)]$ are specified in the bottom panel. In (b) the evolution of the phonon spectra is plotted presenting the results at iterations B, D, and F, together with the starting harmonic phonon spectra.

ter applying symmetries, this gives us $N_p = 25$ parameters to be optimized. The difference between the SSCHA force-constants matrix and the harmonic force-constants matrix in the $2 \times 2 \times 1$ supercell is interpolated to the larger $6 \times 6 \times 4$ supercell. Then, the harmonic $6 \times 6 \times 4$ force-constants matrix is added to the result yielding the SSCHA force-constants matrix in the larger $6 \times 6 \times 4$ supercell. The use of a smaller supercell for the SSCHA than for the harmonic case is justified because the difference between the anharmonic and harmonic force-constants matrices is localized in real space.

The starting \mathcal{H}_0 Hamiltonian is the harmonic Hamiltonian and the starting number of configurations $N_c = 20$.

The initial $\Phi(0)$ force-constants matrix of the $2 \times 2 \times 1$ supercell does not have any imaginary eigenvalue. If it was the case, the force-constants matrix should have been modified to avoid initial imaginary frequencies. The minimization is carried out with the following parameters: $\theta = 1$, $\zeta_c = 0.0003$ a.u.² and $\eta = 0.3$. The evolution of the SSCHA calculation is represented in Fig. 2. As it can be seen in Fig. 2(a), the calculation is stopped at $j = A$ when $|\langle \rho_{\mathcal{H}_j} / \rho_{\mathcal{H}_0} \rangle - 1| \geq \eta$. Then, according to the flowchart in Fig. 1, a new set of configurations is created with $N_c = 20$ and the minimization of the free energy continues. New sets of configurations are regenerated at $j = B$, $j = C$ and $j = D$. However, at step $j = E$ the calculation is stopped because all parameters in the gradient satisfy Eq. (41) or Eq. (42) and $n_p = N_p$. The calculation could be stopped here, but in order to increase the accuracy of the result we generate another 380 configurations using $\mathcal{H}_{j=D}$ and calculate total energies and atomic forces for them. Generating these configurations with $\mathcal{H}_{j=D}$ instead of $\mathcal{H}_{j=E}$, we can recycle the previously generated 20 configurations. Thus, the number of configurations is increased up to 400. Then, the minimization restarts till $n_p = N_p$ at step $j = F$. The 400 configurations were enough to converge the phonon spectra. Thus, in total 500 *ab initio* force calculations in supercells containing 16 atoms are needed. One should note that the bulk of the computational effort comes from the *ab initio* calculation of the forces. The other operations of the SSCHA minimization require a negligible computational time.

In Fig. 2 we show as well how the free energy is minimized in the calculation. It is noteworthy that both the harmonic contribution to the free energy, $F_{\mathcal{H}_j}$, and the potential contribution, $\text{tr}[\rho_{\mathcal{H}_j}(V - \mathcal{V}_j)]$, vary a lot in the minimization. At the minimum, at $j = F$, the potential contribution to the free energy is not negligible with respect to the harmonic contribution and it should be taken into account. In Fig. 2(b) the evolution of the phonon spectra during the SSCHA minimization is illustrated.

B. Anharmonic phonon spectra of PtH at 100 GPa

In Fig. 3 we present the phonon spectra calculated in the harmonic approximation and in the SSCHA together with the phonon density of states (PDOS). The obtained harmonic phonon spectra is in good agreement with previous calculations even if we observe a small instability along ΓM not present in previous calculations^{43,65}. The anharmonic correction of the phonon spectra given by the SSCHA is huge. Even if all the modes are affected by anharmonicity, the biggest effect is attributed to the H-character modes with low energy in the harmonic approximation. The small instability present in the harmonic approximation completely disappears in the SSCHA. This suggests that the hcp phase of PtH is stabilized by anharmonic effects down to the pressures where it was observed in experiments⁴⁴, even if harmonic cal-

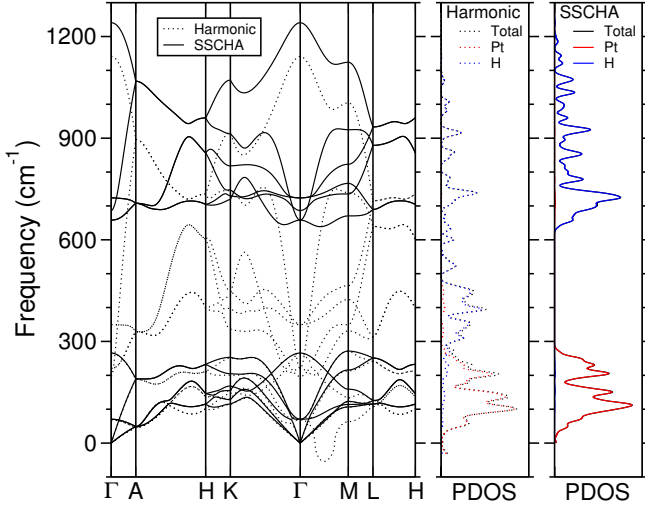


FIG. 3. (Color online) Phonon spectra and PDOS of PtH at 100 GPa and 0 K in the harmonic approximation and in the SSCHA.

culations predict it to be unstable below 100 GPa^{43,65}. This underlines that the SSCHA is a useful method to treat systems that are apparently unstable in the harmonic approximation but are stabilized by anharmonic effects.

It should be stressed that, even if in the harmonic approximation a mixing between H and Pt character is observed in the low-energy modes, the mixing is strongly suppressed in the anharmonic case. This is evident in the projected PDOS shown in Fig. 3. In order to be able to predict this reduction of the mixing, the free energy must be minimized with respect to the polarization vectors. It is unclear how methods like SCAILD^{36,37} and the method presented by Antolin *et al.*³⁸, which as far as we understand do not optimize the polarization vectors, behave in situations where the character of the polarization vectors is strongly altered by anharmonicity as in PtH.

C. Superconductivity of PtH at 100 GPa

Once the phonon spectra renormalized by anharmonicity has been obtained using the SSCHA, anharmonic effects can be easily incorporated into the electron-phonon coupling calculations. Assuming that the main effect of anharmonicity is a change in the phonon frequencies and polarizations, and that the deformation potential is unchanged, the anharmonic Eliashberg function can be calculated as

$$\alpha^2 F(\omega) = \frac{1}{N(0)N_k N_q} \sum_{\mathbf{k}\mathbf{q}\mathbf{n}m} \sum_{\bar{s}\bar{t}\alpha\beta\mu} \frac{\epsilon_{\mu\mathcal{H}}^{\bar{s}\alpha}(\mathbf{q}) \epsilon_{\mu\mathcal{H}}^{\bar{t}\beta*}(\mathbf{q})}{2\omega_{\mu\mathcal{H}}(\mathbf{q}) \sqrt{M_{\bar{s}} M_{\bar{t}}}} \times d_{\mathbf{k}\mathbf{n}, \mathbf{k}+\mathbf{q}m}^{\bar{s}\alpha} d_{\mathbf{k}\mathbf{n}, \mathbf{k}+\mathbf{q}m}^{\bar{t}\beta*} \delta(\epsilon_{\mathbf{k}\mathbf{n}}) \delta(\epsilon_{\mathbf{k}+\mathbf{q}m}) \delta(\omega - \omega_{\mu\mathcal{H}}(\mathbf{q})). \quad (45)$$

In Eq. (45) $d_{\mathbf{k}\mathbf{n}, \mathbf{k}+\mathbf{q}m}^{\bar{s}\alpha} = \langle \mathbf{k}\mathbf{n} | \delta V / \delta u^{\bar{s}\alpha}(\mathbf{q}) | \mathbf{k} + \mathbf{q}m \rangle$ is the deformation potential, $|\mathbf{k}\mathbf{n}\rangle$ is a Kohn-Sham state with

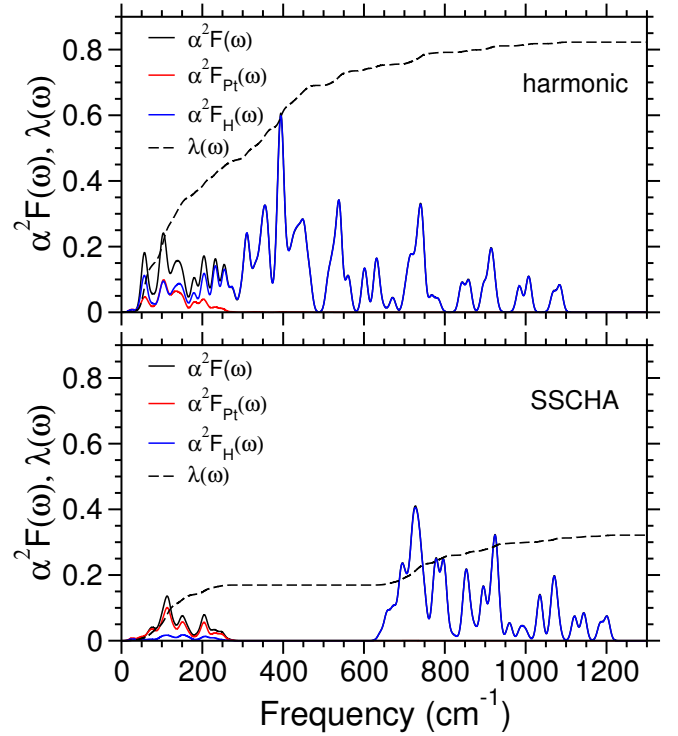


FIG. 4. (Color online) $\alpha^2 F(\omega)$ and $\lambda(\omega)$ of PtH at 100 GPa and 0 K in the harmonic approximation (top panel) and in the SSCHA (bottom panel). The contribution of Pt and H atoms to $\alpha^2 F(\omega)$ is depicted as well.

TABLE I. Calculated λ , ω_{\log} and T_c values for PtH at 100 GPa and 0 K in the harmonic approximation and in the SSCHA.

	λ	$\omega_{\log}(\text{meV})$	$T_c[\mu^* = 0.10](\text{K})$	$T_c[\mu^* = 0.13](\text{K})$
Harmonic	0.82	25.3	14.5	11.8
SSCHA	0.32	36.1	0.4	0.1

energy $\epsilon_{\mathbf{k}\mathbf{n}}$ measured from the Fermi level (ϵ_F), N_k and N_q are the number of electron and phonon momentum points used for the 1BZ sampling, and $N(0)$ is the density of states per spin at ϵ_F . Note that in Eq. (45) the sum over atomic indices is limited to the unit cell so that phonon frequencies and polarization vectors are labeled with a momentum \mathbf{q} . Similarly, $u^{\bar{s}\alpha}(\mathbf{q})$ is the Fourier transform of $u^{s\alpha}$. We have used a finer $60 \times 60 \times 36$ mesh in the sum over \mathbf{k} points in Eq. (45).

The Eliashberg function in the harmonic approximation and in the SSCHA is shown in Fig. 4 together with the integrated electron-phonon coupling constant

$$\lambda(\omega) = 2 \int_0^\omega d\omega' \frac{\alpha^2 F(\omega')}{\omega'}. \quad (46)$$

With the electron-phonon coupling constant λ , $\lambda =$

$\lim_{\omega \rightarrow \infty} \lambda(\omega)$, and the logarithmic frequency average,

$$\omega_{\log} = \exp \left(\frac{2}{\lambda} \int_0^\infty d\omega \frac{\alpha^2 F(\omega)}{\omega} \ln \omega \right), \quad (47)$$

we estimate T_c making use of the Allen-Dynes modified McMillan equation⁶⁶, using $\mu^* = 0.10$ and $\mu^* = 0.13$ for the Coulomb pseudopotential. The results for λ , ω_{\log} and T_c are summarized in Table I. In the harmonic approximation, despite the instability that barely contributes to $\alpha^2 F(\omega)$, we obtain a λ and T_c in agreement with previous calculations⁴³. In the SSCHA, λ is strongly suppressed due to the enhancement of the frequencies induced by anharmonicity. In Fig. 4 we show that the H contribution to the Eliashberg function shifts to higher energies in the SSCHA, highly reducing the H contribution to λ . While in the harmonic approximation H remarkably contributes to $\alpha^2 F(\omega)$ at low energies, this is no longer true in the anharmonic case. This again evidences the fact that the H and Pt mixing of the low-energy modes disappears with anharmonicity.

The suppression in λ makes T_c smaller than 1 K. This means that the superconducting critical temperature is reduced by an order of magnitude in PtH when anharmonicity is included. Even if we do not include anharmonic corrections in the deformation potential, our results indicate that at 100 GPa PtH is not superconducting at around 17 K as measured in the experiment of silane⁴⁶. The interpretation that in the experiment in Ref. 46 the superconductivity of PtH was measured is therefore questioned by our calculations.

V. APPLICATION OF THE STOCHASTIC SELF-CONSISTENT HARMONIC APPROXIMATION TO PALLADIUM HYDRIDES

Secondly, we apply the SSCHA to the strongly anharmonic palladium hydrides. In palladium hydrides the anharmonic correction of the phonon frequencies is larger than the harmonic frequencies themselves, invalidating any perturbative approach as we have demonstrated recently in Ref. 25. The harmonic approximation displays imaginary phonon frequencies for lattice parameters larger than approximately 7.72 a.u. Considering that experimental lattice parameters of palladium hydrides are around 7.73 a.u.^{67,68}, the quasi-harmonic approximation is not valid to study thermodynamic properties as the harmonic energy has no lower bound in case imaginary phonons are present. Moreover, the harmonic approximation strongly overestimates superconducting transition temperatures in palladium hydrides and, obviously, does not explain the inversion of the isotope effect⁶⁹⁻⁷¹. In Ref. 25 we showed how the SSCHA explains the dynamical stability of palladium hydrides, the thermal expansion and even the inverse isotope effect. Here we describe in further detail the thermodynamic properties of PdH, PdD and PdT.

A. Calculation details

In the calculations presented here we make use of a model potential built on top of first-principles calculations that combines the *ab initio* harmonic potential with a fourth-order on-site anharmonic potential. The reader is referred to Ref. 25 for the details of the model potential and the SSCHA calculation. The model potential allows us to reduce the statistical noise in the calculation of the free energy. We calculate the free energy of PdH, PdD and PdT at several volumes and temperatures. The vibrational contribution to the free energy is a smooth function of the volume that can be fitted accurately to a low order polynomial. We use a second order polynomial to fit these contributions. Then, the electronic ground state energy is added to the vibrational free energy to obtain the total free energy. From the minimum of the free energy at each temperature we calculate the dependence of the lattice parameter as a function of temperature and the value of the free energy at zero pressure for each isotope.

B. Thermodynamic properties

In Fig. 5 we plot the total free energy at zero pressure and the equilibrium lattice parameter for PdH, PdD and PdT as a function of temperature. As it was shown in Ref. 25, the results obtained for the lattice parameter are in close agreement with experiments^{67,68}. Here we note that in the case of palladium hydrides the inclusion of $\text{tr}[\rho_{\mathcal{H}}(V - \mathcal{V})]$ in Eq. (10), which gives the vibrational free energy, is crucial to account for thermodynamic properties. As it happens in PtH (see Fig. 2) at the minimum this potential contribution is not negligible. Indeed, as shown in Fig. 5 the total free energy is systematically overestimated if it is calculated considering exclusively $F_{\mathcal{H}}$ for the vibrational contribution. The overestimation is more important the higher the temperature and the lighter the isotope. In the lattice parameter the effect is very remarkable since at 600 K, for example, neglecting the potential contribution $\text{tr}[\rho_{\mathcal{H}}(V - \mathcal{V})]$ the lattice parameter is underestimated by 0.026 a.u. for PdH. Thus, we can conclude that in palladium hydrides neglecting $\text{tr}[\rho_{\mathcal{H}}(V - \mathcal{V})]$ is not a good approximation. For strongly anharmonic systems a similar behavior is expected.

We should note that, as far as we understand, the SCAILD method^{36,37} and the method presented by Antolin *et al.*³⁸ do not include the $\text{tr}[\rho_{\mathcal{H}}(V - \mathcal{V})]$ potential contribution in the free energy. On the contrary, in the SSCHA we can accurately calculate this contribution without applying thermodynamic integration, which is the way it can be incorporated in the TDEP method⁴⁰.

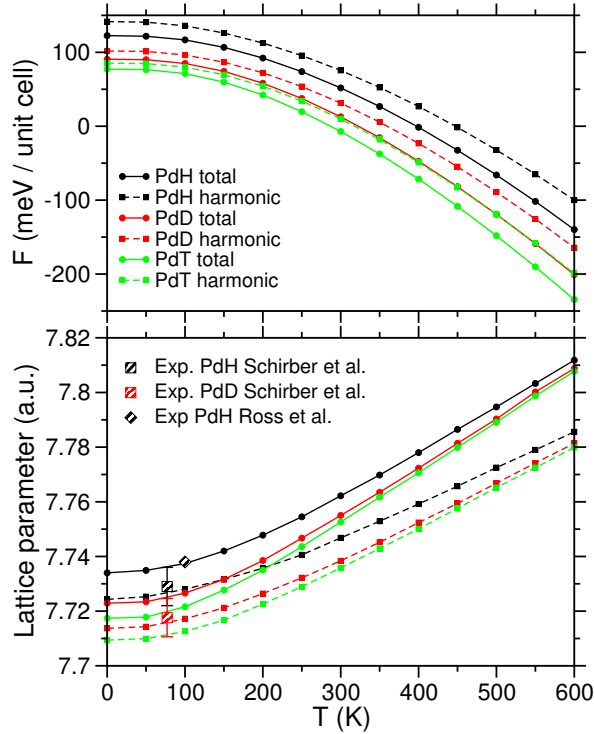


FIG. 5. (Color online) Total free energy at zero pressure (top panel) and the lattice parameter (bottom panel) as a function of temperature for PdH, PdD and PdT. In both figures circles with solid lines represent data obtained with $\mathcal{F}_H[\mathcal{H}]$ for the total vibrational contribution, while squares with dashed lines represent data with exclusively the harmonic contribution F_H for the vibrational contribution. Experimental lattice parameters obtained by Schirber *et al.*⁶⁷ and Ross *et al.*⁶⁸ are included.

VI. CONCLUSIONS

The development of a non-perturbative treatment of anharmonic corrections to the phonon frequencies and the free energy is a major challenge with impacts in many domains of physics and chemistry, including superconductivity, charge-density waves, thermoelectric materials, ferroelectrics, thermodynamic phase transitions and many more. In this work we solve this issue by developing the stochastic self-consistent harmonic approximation. This method is non-perturbative and scales favorably with the system size as it can benefit from the locality of the anharmonic contribution to the forces acting on the atoms. It is variational in the free energy at any temperature as it minimizes it with respect to a trial harmonic density matrix. The gradient of the free energy is calculated as a function of all the independent parameters in the trial harmonic Hamiltonian, and, thus, the SSCHA can calculate the equilibrium positions, phonon frequencies and polarizations vectors beyond perturbation theory. The gradient of the free energy is calculated stochastically from total energies and atomic forces on supercells with ionic configurations described by the

probability distribution defined by the trial Hamiltonian. Therefore, the SSCHA can be applied at different degrees of theory using different total-energy-force engines, e.g., classical potentials, *ab initio* DFT approaches, or Quantum Monte Carlo (QMC). The SSCHA scheme is devised to minimize the number of calls to the total-energy-force engine. The algorithm is such that all the computer time goes in the calculation of total energies and forces if a DFT approach or a more precise approach like QMC is followed.

We apply the method to platinum hydride at high-pressure and palladium hydrides. In the case of palladium hydrides we demonstrate how within the SSCHA we can calculate thermodynamic properties in agreement with experiments even when the quasiharmonic approximation breaks down. In PtH, we have reanalyzed the phonon spectra and its superconducting properties at 100 GPa. We have shown that anharmonicity strongly renormalizes the phonon frequencies beyond the perturbative regime with a considerable suppression of the superconducting critical temperature with respect to previous harmonic estimates^{43–45}. This result makes us wonder whether the interpretation that in the experiment in silane by Eremets *et al.*⁴⁶ the superconductivity of PtH was measured^{43–45} is valid. Considering the similar suppression in palladium hydrides, which explains its inverse isotope effect²⁵, and the lack of superconductivity measured in AlH₃ despite been predicted within the harmonic theory^{8,72}, it seems that anharmonicity might strongly affect the predicted T_c values in several hydrides^{8,43,58–62}.

ACKNOWLEDGMENTS

I.E. would like to acknowledge financial support from the Department of Education, Language Policy and Culture of the Basque Government (Grant No. BFI-2011-65). The authors acknowledge support from the Graphene Flagship and from the French state funds managed by the ANR within the Investissements d’Avenir programme under reference ANR-11-IDEX-0004-02, ANR-11-BS04-0019 and ANR-13-IS10-0003-01. Computer facilities were provided by CINES, CCRT and IDRIS (Project No. x2014091202).

Appendix A: Calculation of the gradient of the free energy

In order to calculate the derivatives of $\mathcal{F}_H[\mathcal{H}]$, it is convenient to work with normal coordinates. The quantum statistical average of an operator that exclusively depends on atomic positions can be calculated in normal coordinates applying the change of variables defined in

Eq. (13) to Eq. (18), namely

$$\text{tr}[\rho_{\mathcal{H}}O] = \int d\mathbf{q} O(\dots, R_{\text{eq}}^{s\alpha} + \sum_{\mu=1}^{3N} \frac{1}{\sqrt{M_s}} \epsilon_{\mu\mathcal{H}}^{s\alpha} q_{\mu}, \dots) \rho_{\mathcal{H}}(\mathbf{q}), \quad (\text{A1})$$

where \mathbf{q} is a general configuration of the normal coordinates and $\rho_{\mathcal{H}}(\mathbf{q})$ is the probability to find the system in the configuration \mathbf{q} . In normal coordinates, $\rho_{\mathcal{H}}(\mathbf{q})$ is nothing but a product of Gaussians⁷³:

$$\rho_{\mathcal{H}}(\mathbf{q}) = \prod_{\mu=1}^{3N} \frac{1}{a_{\mu\mathcal{H}} \sqrt{2\pi}} e^{-\frac{q_{\mu}^2}{2a_{\mu\mathcal{H}}^2}}. \quad (\text{A2})$$

If we make use of the $y_{\mu} = q_{\mu}/a_{\mu\mathcal{H}}$ change of variables, the integral can be written as

$$\begin{aligned} \text{tr}[\rho_{\mathcal{H}}O] &= \int d\mathbf{y} O(\dots, R_{\text{eq}}^{s\alpha} + \sum_{\mu=1}^{3N} \frac{1}{\sqrt{M_s}} \epsilon_{\mu\mathcal{H}}^{s\alpha} a_{\mu\mathcal{H}} y_{\mu}, \dots) \\ &\times \prod_{\mu=1}^{3N} \frac{1}{\sqrt{2\pi}} e^{-\frac{y_{\mu}^2}{2}}, \end{aligned} \quad (\text{A3})$$

where \mathbf{y} represents all the set of y_{μ} 's. Writing the quantum statistical average in this way, the exponential part becomes independent of phonon frequencies, polarization vectors and equilibrium positions.

The only non analytic part in the calculation of $\mathcal{F}_H[\mathcal{H}] = F_{\mathcal{H}} + \text{tr}[\rho_{\mathcal{H}}(V - \mathcal{V})]$ is the quantum statistical average of the potential, the $\text{tr}[\rho_{\mathcal{H}}V]$ term. The analytic expression of $F_{\mathcal{H}}$ is given in Eq. (19) and

$$\text{tr}[\rho_{\mathcal{H}}\mathcal{V}] = \sum_{\mu=1}^{3N} \frac{1}{2} \omega_{\mu\mathcal{H}}^2 a_{\mu\mathcal{H}}^2. \quad (\text{A4})$$

Before we demonstrate Eqs. (21) and (22), we also would like to note the following analytical relation involving the $\mathbf{f}_{\mathcal{H}}(\mathbf{R})$ harmonic forces:

$$\begin{aligned} \int d\mathbf{R} f_{\mathcal{H}}^{s\alpha}(\mathbf{R}) (R^{t\beta} - R_{\text{eq}}^{t\beta}) \rho_{\mathcal{H}}(\mathbf{R}) &= \\ - \sum_{\mu=1}^{3N} \sqrt{\frac{M_s}{M_t}} \epsilon_{\mu\mathcal{H}}^{s\alpha} \epsilon_{\mu\mathcal{H}}^{t\beta} \omega_{\mu\mathcal{H}}^2 a_{\mu\mathcal{H}}^2. \end{aligned} \quad (\text{A5})$$

First of all, if we write $\text{tr}[\rho_{\mathcal{H}}V]$ as in Eq. (A3), it is easy to observe that

$$\nabla_{\mathbf{R}_{\text{eq}}} \mathcal{F}_H[\mathcal{H}] = \nabla_{\mathbf{R}_{\text{eq}}} \text{tr}[\rho_{\mathcal{H}}V] = - \int d\mathbf{R} \mathbf{f}(\mathbf{R}) \rho_{\mathcal{H}}(\mathbf{R}). \quad (\text{A6})$$

Noting that $\int d\mathbf{R} \mathbf{f}_{\mathcal{H}}(\mathbf{R}) \rho_{\mathcal{H}}(\mathbf{R}) = 0$, we recover Eq. (21).

Secondly, we calculate $\nabla_{\Phi} \mathcal{F}_H[\mathcal{H}]$ using the chain rule as

$$\nabla_{\Phi} \mathcal{F}_H[\mathcal{H}] = \sum_{\mu} \frac{\partial \mathcal{F}_H[\mathcal{H}]}{\partial a_{\mu\mathcal{H}}} \nabla_{\Phi} a_{\mu\mathcal{H}} + \sum_{\mu s \alpha} \frac{\partial \mathcal{F}_H[\mathcal{H}]}{\partial \epsilon_{\mu\mathcal{H}}^{s\alpha}} \nabla_{\Phi} \epsilon_{\mu\mathcal{H}}^{s\alpha}. \quad (\text{A7})$$

The partial derivative with respect to the polarization vectors is easily obtained writing again $\text{tr}[\rho_{\mathcal{H}}V]$ as in Eq. (A3). In particular,

$$\begin{aligned} \frac{\partial \mathcal{F}_H[\mathcal{H}]}{\partial \epsilon_{\mu\mathcal{H}}^{s\alpha}} &= \frac{\partial \text{tr}[\rho_{\mathcal{H}}V]}{\partial \epsilon_{\mu\mathcal{H}}^{s\alpha}} = - \sum_{t\beta} \sqrt{\frac{M_t}{M_s}} \epsilon_{\mu\mathcal{H}}^{t\beta} \\ &\times \int d\mathbf{R} f_{\mathcal{H}}^{s\alpha}(\mathbf{R}) (R^{t\beta} - R_{\text{eq}}^{t\beta}) \rho_{\mathcal{H}}(\mathbf{R}). \end{aligned} \quad (\text{A8})$$

Making use of Eq. (A5) we can write

$$\begin{aligned} \frac{\partial \mathcal{F}_H[\mathcal{H}]}{\partial \epsilon_{\mu\mathcal{H}}^{s\alpha}} &= \epsilon_{\mu\mathcal{H}}^{s\alpha} \omega_{\mu\mathcal{H}}^2 a_{\mu\mathcal{H}}^2 - \sum_{t\beta} \sqrt{\frac{M_t}{M_s}} \epsilon_{\mu\mathcal{H}}^{t\beta} \\ &\times \int d\mathbf{R} [f_{\mathcal{H}}^{s\alpha}(\mathbf{R}) - f_{\mathcal{H}}^{s\alpha}(\mathbf{R})] (R^{t\beta} - R_{\text{eq}}^{t\beta}) \rho_{\mathcal{H}}(\mathbf{R}). \end{aligned} \quad (\text{A9})$$

On the other hand,

$$\frac{\partial \mathcal{F}_H[\mathcal{H}]}{\partial a_{\mu\mathcal{H}}} = \frac{\partial (F_{\mathcal{H}} - \text{tr}[\rho_{\mathcal{H}}\mathcal{V}])}{\partial a_{\mu\mathcal{H}}} + \frac{\partial \text{tr}[\rho_{\mathcal{H}}V]}{\partial a_{\mu\mathcal{H}}} \quad (\text{A10})$$

It is straightforward to demonstrate that

$$\begin{aligned} \frac{\partial \text{tr}[\rho_{\mathcal{H}}V]}{\partial a_{\mu\mathcal{H}}} &= - \sum_{st\alpha\beta} \sqrt{\frac{M_t}{M_s}} \epsilon_{\mu\mathcal{H}}^{s\alpha} \epsilon_{\mu\mathcal{H}}^{t\beta} \frac{1}{a_{\mu\mathcal{H}}} \\ &\times \int d\mathbf{R} f_{\mathcal{H}}^{s\alpha}(\mathbf{R}) (R^{t\beta} - R_{\text{eq}}^{t\beta}) \rho_{\mathcal{H}}(\mathbf{R}) \end{aligned} \quad (\text{A11})$$

if Eq. (A3) is used to write the quantum statistical average. Using Eq. (A5) the equation above can be rewritten as

$$\begin{aligned} \frac{\partial \text{tr}[\rho_{\mathcal{H}}V]}{\partial a_{\mu\mathcal{H}}} &= \omega_{\mu\mathcal{H}}^2 a_{\mu\mathcal{H}} - \sum_{st\alpha\beta} \sqrt{\frac{M_t}{M_s}} \epsilon_{\mu\mathcal{H}}^{s\alpha} \epsilon_{\mu\mathcal{H}}^{t\beta} \frac{1}{a_{\mu\mathcal{H}}} \\ &\times \int d\mathbf{R} [f_{\mathcal{H}}^{s\alpha}(\mathbf{R}) - f_{\mathcal{H}}^{s\alpha}(\mathbf{R})] (R^{t\beta} - R_{\text{eq}}^{t\beta}) \rho_{\mathcal{H}}(\mathbf{R}) \end{aligned} \quad (\text{A12})$$

Finally, plugging Eqs. (A12) and (A9) into Eq. (A7), and noting that

$$\frac{\partial (F_{\mathcal{H}} - \text{tr}[\rho_{\mathcal{H}}\mathcal{V}])}{\partial a_{\mu\mathcal{H}}} + \omega_{\mu\mathcal{H}}^2 a_{\mu\mathcal{H}} = 0 \quad (\text{A13})$$

$$\sum_{s\alpha} \epsilon_{\mu\mathcal{H}}^{s\alpha} \nabla_{\Phi} \epsilon_{\mu\mathcal{H}}^{s\alpha} = 0, \quad (\text{A14})$$

it is straightforward to obtain the expression for $\nabla_{\Phi} \mathcal{F}_H[\mathcal{H}]$ given in Eq. (22).

The only elements contributing to $\nabla_{\Phi} \mathcal{F}_H[\mathcal{H}]$ that have not been specified yet are $\nabla_{\Phi} a_{\mu\mathcal{H}}$ and $\nabla_{\Phi} \epsilon_{\mu\mathcal{H}}^{s\alpha}$. Considering how eigenvalues and eigenvectors of a matrix are modified when the matrix itself is varied, we can get the following expressions for the components of these gradients:

$$\frac{\partial a_{\mu\mathcal{H}}}{\partial \Phi_{st}^{\alpha\beta}} = \frac{\partial a_{\mu\mathcal{H}}}{\partial \omega_{\mu\mathcal{H}}} \frac{1}{2\omega_{\mu\mathcal{H}}} \frac{\epsilon_{\mu\mathcal{H}}^{s\alpha} \epsilon_{\mu\mathcal{H}}^{t\beta}}{\sqrt{M_s M_t}} \quad (\text{A15})$$

$$\frac{\partial \epsilon_{\mu\mathcal{H}}^{s\alpha}}{\partial \Phi_{kt}^{\gamma\beta}} = \sum_{\nu, \nu \neq \mu} \frac{\epsilon_{\nu\mathcal{H}}^{k\gamma} \epsilon_{\mu\mathcal{H}}^{t\beta}}{\sqrt{M_k M_t} (\omega_{\mu\mathcal{H}}^2 - \omega_{\nu\mathcal{H}}^2)} \epsilon_{\nu\mathcal{H}}^{s\alpha}. \quad (\text{A16})$$

The $\partial a_{\mu\mathcal{H}}/\partial \omega_{\mu\mathcal{H}}$ derivative in Eq. (A15) can be obtained from Eq. (17).

Appendix B: Symmetrization and reduction of the basis for the force-constants matrix

In order to apply \hat{S} and time-reversal symmetries to the $\{\mathcal{G}_{(\text{ns})}(m)\}_{m=1,\dots,(3n)^2 N_1 N_2 N_3}$ basis, it is convenient to work in the unit-cell phonon-momentum \mathbf{q} space. This is so because any Φ force-constants matrix of this vector space respects translational symmetries and, thus, its Fourier transform can be labeled with a single \mathbf{q} vector of the 1BZ of the unit cell. The number of \mathbf{q} points in the 1BZ is determined by the supercell size. A $N_1 \times N_2 \times N_3$ supercell means a $N_1 \times N_2 \times N_3$ phonon-momentum grid in the 1BZ of the unit cell. The Fourier components of the real-space force-constants matrix of the supercell Φ are labeled as $\Phi(\mathbf{q})$. Each $\Phi(\mathbf{q})$ is a $3n \times 3n$ Hermitian matrix. Therefore, in practice we do not work with the vector space defined by the $\{\mathcal{G}_{(\text{ns})}(m)\}_{m=1,\dots,(3n)^2 N_1 N_2 N_3}$ basis, but with the vector space formed by the $3n \times 3n$ Hermitian matrices. The dimension of this vector space is $(3n)^2$ and let $\{\bar{\mathcal{G}}_{(\text{ns})}(\sigma)\}_{\sigma=1,\dots,(3n)^2}$ be an orthonormal basis of it. The elements of the basis satisfy the orthonormality condition defined in Eq. (30). Therefore, any $\Phi(\mathbf{q})$ can be decomposed in this basis as

$$\Phi(\mathbf{q}) = \sum_{\sigma=1}^{(3n)^2} c_{(\text{ns})}(\mathbf{q}, \sigma) \bar{\mathcal{G}}_{(\text{ns})}(\sigma), \quad (\text{B1})$$

where the $c_{(\text{ns})}(\mathbf{q}, \sigma)$ coefficients determine the value of $\Phi(\mathbf{q})$.

Any $\Phi(\mathbf{q})$ matrix described in the $\{\bar{\mathcal{G}}_{(\text{ns})}(\sigma)\}_{\sigma=1,\dots,(3n)^2}$ basis as in Eq. (B1) transforms under the symmetry operations \hat{S} of the space group as

$$\Phi(S\mathbf{q}) = T_{\hat{S}}(\mathbf{q}) \Phi(\mathbf{q}) T_{\hat{S}}^\dagger(\mathbf{q}), \quad (\text{B2})$$

where the unitary $T_{\hat{S}}(\mathbf{q})$ matrices are given in Refs. 51, 74, and 75. Eq. (B2) shows that many of the \mathbf{q} points in the $N_1 \times N_2 \times N_3$ mesh are equivalent by symmetry since the force-constants matrices at $S\mathbf{q}$ points of the 1BZ are related by symmetry to the force-constants matrix at \mathbf{q} . The set of symmetry related $S\mathbf{q}$ points is named as the star of \mathbf{q} and we denote it as $\{\mathbf{q}^*\}$. The \mathbf{q} points not related by Eq. (B2) form the irreducible Brillouin zone (IBZ). Therefore, we can restrict the $\Phi(\mathbf{q})$ Fourier-components of the supercell force-constants matrix at the \mathbf{q} points in the IBZ. Indeed, all the $N_1 \times N_2 \times N_3$ $\Phi(\mathbf{q})$ matrices can be generated by symmetry using Eq. (B2).

Eq. (B2) can be used to symmetrize the elements of the $\{\bar{\mathcal{G}}_{(\text{ns})}(\sigma)\}_{\sigma=1,\dots,(3n)^2}$ basis with respect to the \hat{S} operations and time-reversal. For instance, if

$$S_{\mathbf{q}}\mathbf{q} = \mathbf{q} + \mathbf{G}_{\mathbf{q}} \quad (\text{B3})$$

or

$$S_{-\mathbf{q}}\mathbf{q} = -\mathbf{q} + \mathbf{G}_{-\mathbf{q}}, \quad (\text{B4})$$

we can use the $\hat{S}_{\mathbf{q}}$ and $\hat{S}_{-\mathbf{q}}$ symmetry operations to symmetrize the basis. The $\hat{S}_{\mathbf{q}}$ symmetry operations form

the so-called small group of \mathbf{q} . The $\hat{S}_{-\mathbf{q}}$ operations can be used to symmetrize the basis because of time-reversal symmetry. From Eq. (B2) it is straightforward to observe that the elements of the basis can be symmetrized as

$$\begin{aligned} \bar{\mathcal{G}}_{(\text{s})}(\mathbf{q}, \sigma) &= \frac{1}{N_{S_{\mathbf{q}}}} \sum_{\hat{S}_{\mathbf{q}}} T_{\hat{S}_{\mathbf{q}}}^\dagger(\mathbf{q}) \bar{\mathcal{G}}_{(\text{ns})}(\sigma) T_{\hat{S}_{\mathbf{q}}}(\mathbf{q}) \\ &+ \frac{1}{N_{S_{-\mathbf{q}}}} \sum_{\hat{S}_{-\mathbf{q}}} T_{\hat{S}_{-\mathbf{q}}}^\dagger(\mathbf{q}) \bar{\mathcal{G}}_{(\text{ns})}^*(\sigma) T_{\hat{S}_{-\mathbf{q}}}(\mathbf{q}), \end{aligned} \quad (\text{B5})$$

where $N_{S_{\mathbf{q}}}$ is the number symmetry operations in the small group of \mathbf{q} and $N_{S_{-\mathbf{q}}}$ the number of symmetry operations satisfying Eq. (B4). We perform this symmetrization at each $\mathbf{q} \in \text{IBZ}$. The $\{\bar{\mathcal{G}}_{(\text{s})}(\mathbf{q}, \sigma)\}_{\sigma=1,\dots,(3n)^2}$ basis becomes overcomplete after the symmetrization. We reduce the basis applying a Gram-Schmidt orthonormalization procedure. We label the set of matrices that form the basis of the symmetrized subspace as $\{\bar{\mathcal{G}}(\mathbf{q}, \sigma)\}_{\sigma=1,\dots,N_r(\mathbf{q})}$, $N_r(\mathbf{q})$ being the dimension of the subspace for $\mathbf{q} \in \text{IBZ}$.

In this framework, it is also easy to impose the acoustic sum rule (ASR) as among the $\bar{\mathcal{G}}_{(\text{s})}(\Gamma, \sigma)$ matrices there must exist three translation generators, one for each Cartesian direction: \mathcal{G}_t^x , \mathcal{G}_t^y and \mathcal{G}_t^z . According to the ASR, the translation vectors must be eigenvectors of the force-constants matrix at Γ with vanishing eigenvalue. In order to impose this property, we redefine all the generators at Γ according to the

$$\bar{\mathcal{G}}_{\text{ASR}}(\Gamma, \sigma) = (\mathbb{I} - \mathcal{G}_t) \bar{\mathcal{G}}_{(\text{s})}(\Gamma, \sigma) (\mathbb{I} - \mathcal{G}_t) \quad (\text{B6})$$

projection, where \mathbb{I} is the identity matrix and $\mathcal{G}_t = \mathcal{G}_t^x + \mathcal{G}_t^y + \mathcal{G}_t^z$. Then, instead of performing the Gram-Schmidt orthonormalization in the $\{\bar{\mathcal{G}}_{(\text{s})}(\Gamma, \sigma)\}_{\sigma=1,\dots,(3n)^2}$ basis, we perform it in the $\{\bar{\mathcal{G}}_{\text{ASR}}(\Gamma, \sigma)\}_{\sigma=1,\dots,(3n)^2}$ one. This procedure gives us the $\{\bar{\mathcal{G}}(\Gamma, \sigma)\}_{\sigma=1,\dots,N_r(\Gamma)}$ basis of the symmetric subspace at Γ .

Once the symmetry reduced basis is found for all $\mathbf{q} \in \text{IBZ}$, we decompose the initial force-constants matrix $\Phi(0)$ in the basis. In order to decompose it, it is sufficient to decompose the Fourier transformed force-constants matrices at $\mathbf{q} \in \text{IBZ}$. The decomposition of each of these matrices is given as

$$\Phi(\mathbf{q}, 0) = \sum_{\sigma=1}^{N_r(\mathbf{q})} c_0(\mathbf{q}, \sigma) \bar{\mathcal{G}}(\mathbf{q}, \sigma), \quad (\text{B7})$$

where the $c_0(\mathbf{q}, \sigma)$ coefficients can be obtain from the

$$c_0(\mathbf{q}, \sigma) = \langle \Phi(\mathbf{q}, 0), \bar{\mathcal{G}}(\mathbf{q}, \sigma) \rangle \quad (\text{B8})$$

scalar product. The scalar product in Eq. (B8) is defined in Eq. (29) though, in this case, the sum over atom indices is limited to the unit cell. It is clear that the total number of coefficients needed to determine $\Phi(0)$, or in general any $\Phi(j)$, is $N_R = \sum_{\mathbf{q} \in \text{IBZ}} N_r(\mathbf{q})$.

Finally, in order to obtain Eq. (32), we need to Fourier transform to real space the $\tilde{\mathcal{G}}(\mathbf{q}, \sigma)$ matrices. The $\tilde{\mathcal{G}}(\mathbf{q}', \sigma)$ matrices for all $\mathbf{q}' \in \{\mathbf{q}^*\}$ can be obtained using Eq. (B2). The

$$\mathcal{G}_{st}^{\alpha\beta}(\mathbf{q}, \sigma) = \frac{1}{N_q} \sum_{\mathbf{q}' \in \{\mathbf{q}^*\}} \tilde{\mathcal{G}}_{\bar{s}\bar{t}}^{\alpha\beta}(\mathbf{q}', \sigma) e^{i\mathbf{q}'(\mathbf{R}_{s\bar{s}} - \mathbf{R}_{t\bar{t}})} \quad (\text{B9})$$

Fourier transform gives us the value of the matrix in real space. In Eq. (B9) $N_q = N_1 \times N_2 \times N_3$ is the total number of \mathbf{q} points in the 1BZ and $\mathbf{R}_{s\bar{s}}$ is the lattice vector that connects the s -th atom of the supercell with the equivalent atom \bar{s} in the unit cell, $\mathbf{R}_{s\bar{s}} = \mathbf{R}_{\text{eq}}^s - \mathbf{R}_{\text{eq}}^{\bar{s}}$. Note that $\mathcal{G}_{st}^{\alpha\beta}(\mathbf{q}, \sigma)$ denotes an element of the symmetrized basis in real space and that \mathbf{q}, σ is nothing but the label of a matrix in the basis. Moreover, as for $\mathbf{q}' \in \{\mathbf{q}^*\}$ $c_0(\mathbf{q}', \sigma) = c_0(\mathbf{q}, \sigma)$, the $\Phi(0)$ force-constants matrix in real space can be calculated as

$$\Phi_{st}^{\alpha\beta}(0) = \sum_{\mathbf{q} \in \text{IBZ}} \sum_{\sigma=1}^{N_r(\mathbf{q})} c_0(\mathbf{q}, \sigma) \mathcal{G}_{st}^{\alpha\beta}(\mathbf{q}, \sigma). \quad (\text{B10})$$

Simplifying the notation as $m \equiv \mathbf{q}, \sigma$ we get

$$\Phi(0) = \sum_{m=1}^{N_R} c_0(m) \mathcal{G}(m), \quad (\text{B11})$$

where the sum runs over the N_R different coefficients. Obviously at CG step j Eq. (B11) holds as in Eq. (32).

Appendix C: Creating the set of ionic configurations

In order to create the $\{\mathbf{R}_I\}_{I=1, \dots, N_c}$ set of ionic configurations according to the probability distribution $\rho_{\mathcal{H}}(\mathbf{R})$, we take advantage of the Gaussian character of $\rho_{\mathcal{H}}(\mathbf{q})$ (see Eq. (A2)). First of all, a set of $\{y_{\mu I}\}_{I=1, \dots, N_c}$ configurations is created. Each $y_{\mu I}$ is a random number created according to a purely Gaussian distribution. Then, we multiply each $y_{\mu I}$ by the corresponding $a_{\mu \mathcal{H}}$ normal length. This operation gives us a set of configurations for the normal coordinates described by the $\rho_{\mathcal{H}}(\mathbf{q})$ probability distribution: $\{q_{\mu I} = a_{\mu \mathcal{H}} y_{\mu I}\}_{I=1, \dots, N_c}$. From Eq. (13), these normal coordinates define a set of configurations for the ionic positions $\{\mathbf{R}_I\}_{I=1, \dots, N_c}$, where each component is given as

$$R_I^{s\alpha} = R_{\text{eq}}^{s\alpha} + \sum_{\mu=1}^{3N} \frac{1}{\sqrt{M_s}} \epsilon_{\mu \mathcal{H}}^{s\alpha} a_{\mu \mathcal{H}} y_{\mu I}. \quad (\text{C1})$$

-
- ¹ M. Born and K. Huang, *Dynamical Theory of Crystal Lattices* (Oxford University Press, Oxford, 1954).
 - ² S. Baroni, S. de Gironcoli, A. Dal Corso, and P. Giannozzi, *Rev. Mod. Phys.* **73**, 515 (2001).
 - ³ G. Kresse, J. Furthmüller, and J. Hafner, *EPL (Europhysics Letters)* **32**, 729 (1995).
 - ⁴ B. Fultz, *Progress in Materials Science* **55**, 247 (2010).
 - ⁵ A. A. Maradudin and A. E. Fein, *Phys. Rev.* **128**, 2589 (1962).
 - ⁶ M. Lazzeri, M. Calandra, and F. Mauri, *Phys. Rev. B* **68**, 220509 (2003).
 - ⁷ M. Lazzeri and S. de Gironcoli, *Phys. Rev. B* **65**, 245402 (2002).
 - ⁸ B. Rousseau and A. Bergara, *Phys. Rev. B* **82**, 104504 (2010).
 - ⁹ L. Paulatto, F. Mauri, and M. Lazzeri, *Phys. Rev. B* **87**, 214303 (2013).
 - ¹⁰ D. J. Hooton, *Philosophical Magazine Series 7* **46**, 422 (1955).
 - ¹¹ I. Errea, B. Rousseau, and A. Bergara, *Journal of Physics: Conference Series* **377**, 012060 (2012).
 - ¹² I. Errea, B. Rousseau, and A. Bergara, *Phys. Rev. Lett.* **106**, 165501 (2011).
 - ¹³ G. Profeta, C. Franchini, N. N. Lathiotakis, A. Floris, A. Sanna, M. A. L. Marques, M. Lüders, S. Massidda, E. K. U. Gross, and A. Continenza, *Phys. Rev. Lett.* **96**, 047003 (2006).
 - ¹⁴ F. Mauri, O. Zakharov, S. de Gironcoli, S. G. Louie, and M. L. Cohen, *Phys. Rev. Lett.* **77**, 1151 (1996).
 - ¹⁵ O. Degtyareva, M. V. Magnitskaya, J. Kohanoff, G. Profeta, S. Scandolo, M. Hanfland, M. I. McMahon, and E. Gregoryanz, *Phys. Rev. Lett.* **99**, 155505 (2007).
 - ¹⁶ Z. P. Yin, S. Y. Savrasov, and W. E. Pickett, *Phys. Rev. B* **74**, 094519 (2006).
 - ¹⁷ M. Leroux, M. Le Tacon, M. Calandra, L. Cario, M.-A. Méasson, P. Diener, E. Borrisenko, A. Bosak, and P. Rodière, *Phys. Rev. B* **86**, 155125 (2012).
 - ¹⁸ M. Calandra, I. I. Mazin, and F. Mauri, *Phys. Rev. B* **80**, 241108 (2009).
 - ¹⁹ M. Calandra and F. Mauri, *Phys. Rev. Lett.* **106**, 196406 (2011).
 - ²⁰ M. D. Johannes and I. I. Mazin, *Phys. Rev. B* **77**, 165135 (2008).
 - ²¹ M. D. Johannes, I. I. Mazin, and C. A. Howells, *Phys. Rev. B* **73**, 205102 (2006).
 - ²² O. Delaire, J. Ma, K. Marty, A. F. May, M. A. McGuire, M.-H. Du, D. J. Singh, A. Podlesnyak, G. Ehlers, M. D. Lumsden, and B. C. Sales, *Nat. Mater.* **10**, 614 (2011).
 - ²³ W. Zhong, D. Vanderbilt, and K. M. Rabe, *Phys. Rev. B* **52**, 6301 (1995).
 - ²⁴ R. Yu and H. Krakauer, *Phys. Rev. Lett.* **74**, 4067 (1995).
 - ²⁵ I. Errea, M. Calandra, and F. Mauri, *Phys. Rev. Lett.* **111**, 177002 (2013).
 - ²⁶ L. Vocadlo, D. Alfè, M. J. Gillan, I. G. Wood, J. P. Brodholt, and G. D. Price, *Nature* **424**, 536 (2003).
 - ²⁷ W. Luo, B. Johansson, O. Eriksson, S. Arapan, P. Souvatzis, M. I. Katsnelson, and R. Ahuja, *Proc. Natl. Acad. Sci. USA* **107**, 9962 (2010).
 - ²⁸ G. Grimvall, B. Magyari-Köpe, V. Ozoliņš, and K. A. Persson, *Rev. Mod. Phys.* **84**, 945 (2012).
 - ²⁹ T. E. Markland and B. J. Berne, *Proceedings of the National Academy of Sciences* **109**, 7988 (2012).

- ³⁰ R. Car and M. Parrinello, Phys. Rev. Lett. **55**, 2471 (1985).
- ³¹ H. Dammak, Y. Chalopin, M. Laroche, M. Hayoun, and J.-J. Greffet, Phys. Rev. Lett. **103**, 190601 (2009).
- ³² M. Ceriotti, G. Bussi, and M. Parrinello, Phys. Rev. Lett. **103**, 030603 (2009).
- ³³ A. H. Barrozo and M. de Koning, Phys. Rev. Lett. **107**, 198901 (2011).
- ³⁴ H. Dammak, M. Hayoun, Y. Chalopin, and J.-J. Greffet, Phys. Rev. Lett. **107**, 198902 (2011).
- ³⁵ D. M. Ceperley, Rev. Mod. Phys. **67**, 279 (1995).
- ³⁶ P. Souvatzis, O. Eriksson, M. I. Katsnelson, and S. P. Rudin, Phys. Rev. Lett. **100**, 095901 (2008).
- ³⁷ P. Souvatzis, O. Eriksson, M. Katsnelson, and S. Rudin, Computational Materials Science **44**, 888 (2009).
- ³⁸ N. Antolin, O. D. Restrepo, and W. Windl, Phys. Rev. B **86**, 054119 (2012).
- ³⁹ O. Hellman, I. A. Abrikosov, and S. I. Simak, Phys. Rev. B **84**, 180301 (2011).
- ⁴⁰ O. Hellman, P. Steneteg, I. A. Abrikosov, and S. I. Simak, Phys. Rev. B **87**, 104111 (2013).
- ⁴¹ B. Monserrat, N. D. Drummond, and R. J. Needs, Phys. Rev. B **87**, 144302 (2013).
- ⁴² I. Errea, B. Rousseau, and A. Bergara, Journal of Applied Physics **111**, 112604 (2012).
- ⁴³ D. Y. Kim, R. H. Scheicher, C. J. Pickard, R. J. Needs, and R. Ahuja, Phys. Rev. Lett. **107**, 117002 (2011).
- ⁴⁴ T. Scheler, O. Degtyareva, M. Marqués, C. L. Guillaume, J. E. Proctor, S. Evans, and E. Gregoryanz, Phys. Rev. B **83**, 214106 (2011).
- ⁴⁵ X.-F. Zhou, A. R. Oganov, X. Dong, L. Zhang, Y. Tian, and H.-T. Wang, Phys. Rev. B **84**, 054543 (2011).
- ⁴⁶ M. I. Eremets, I. A. Trojan, S. A. Medvedev, J. S. Tse, and Y. Yao, Science **319**, 1506 (2008).
- ⁴⁷ A. Isihara, J. Phys. A: Gen. Phys. **1**, 539 (1968).
- ⁴⁸ R. Choquard, *The anharmonic crystal* (W. A. Benjamin Inc., New York, 1967).
- ⁴⁹ N. R. Werthamer, Phys. Rev. B **1**, 572 (1970).
- ⁵⁰ P. Giannozzi *et al.*, J. Phys. Condens. Matter **21**, 395502 (2009).
- ⁵¹ A. A. Maradudin and S. H. Vosko, Rev. Mod. Phys. **40**, 1 (1968).
- ⁵² G. Lang, K. Karch, M. Schmitt, P. Pavone, A. P. Mayer, R. K. Wehner, and D. Strauch, Phys. Rev. B **59**, 6182 (1999).
- ⁵³ N. Bonini, M. Lazzeri, N. Marzari, and F. Mauri, Phys. Rev. Lett. **99**, 176802 (2007).
- ⁵⁴ At step j of the CG minimization, one could also calculate the integral in Eq. (34) as $\int d\mathbf{R} O(\mathbf{R}) \rho_{\mathcal{H}_j}(\mathbf{R}) \simeq \frac{\langle O \rho_{\mathcal{H}_j} / \rho_{\mathcal{H}_0} \rangle}{\langle \rho_{\mathcal{H}_j} / \rho_{\mathcal{H}_0} \rangle}$. In this case, the error would not be given by Eq. (36), but a slightly modified version. Both ways of calculating the integral become identical in the $N_c \rightarrow \infty$ limit.
- ⁵⁵ H. Hellmann, *Einführung in die Quantumchemie* (Deuticke, 1937).
- ⁵⁶ R. P. Feynman, Phys. Rev. **56**, 340 (1939).
- ⁵⁷ N. W. Ashcroft, Phys. Rev. Lett. **21**, 1748 (1968).
- ⁵⁸ D. Y. Kim, R. H. Scheicher, H.-k. Mao, T. W. Kang, and R. Ahuja, Proc. Natl. Acad. Sci. USA **107**, 2793 (2010).
- ⁵⁹ G. Gao, A. R. Oganov, P. Li, Z. Li, H. Wang, T. Cui, Y. Ma, A. Bergara, A. O. Lyakhov, T. Iitaka, and G. Zou, Proc. Natl. Acad. Sci. USA **107**, 1317 (2010).
- ⁶⁰ G. Gao, A. R. Oganov, A. Bergara, M. Martinez-Canales, T. Cui, T. Iitaka, Y. Ma, and G. Zou, Phys. Rev. Lett. **101**, 107002 (2008).
- ⁶¹ P. Cudazzo, G. Profeta, A. Sanna, A. Floris, A. Continenza, S. Massidda, and E. K. U. Gross, Phys. Rev. Lett. **100**, 257001 (2008).
- ⁶² M. Martinez-Canales, A. R. Oganov, Y. Ma, Y. Yan, A. O. Lyakhov, and A. Bergara, Phys. Rev. Lett. **102**, 087005 (2009).
- ⁶³ O. Degtyareva, J. E. Proctor, C. L. Guillaume, E. Gregoryanz, and M. Hanfland, Solid State Communications **149**, 1583 (2009).
- ⁶⁴ J. P. Perdew, K. Burke, and M. Ernzerhof, Phys. Rev. Lett. **77**, 3865 (1996).
- ⁶⁵ G. Gao, H. Wang, L. Zhu, and Y. Ma, The Journal of Physical Chemistry C **116**, 1995 (2012).
- ⁶⁶ P. B. Allen and R. C. Dynes, Phys. Rev. B **12**, 905 (1975).
- ⁶⁷ J. E. Schirber and B. Morosin, Phys. Rev. B **12**, 117 (1975).
- ⁶⁸ D. K. Ross, V. E. Antonov, E. L. Bokhenkov, A. I. Kolesnikov, E. G. Ponyatovsky, and J. Tomkinson, Phys. Rev. B **58**, 2591 (1998).
- ⁶⁹ B. Stritzker and W. Buckel, Zeitschrift für Physik **257**, 1 (1972).
- ⁷⁰ J. E. Schirber and C. J. M. Northrup, Phys. Rev. B **10**, 3818 (1974).
- ⁷¹ J. E. Schirber, J. M. Mintz, and W. Wall, Solid State Communications **52**, 837 (1984).
- ⁷² I. Goncharenko, M. I. Eremets, M. Hanfland, J. S. Tse, M. Amboage, Y. Yao, and I. A. Trojan, Phys. Rev. Lett. **100**, 045504 (2008).
- ⁷³ S. Rossano, F. Mauri, C. J. Pickard, and I. Farnan, The Journal of Physical Chemistry B **109**, 7245 (2005).
- ⁷⁴ J. L. Warren, Rev. Mod. Phys. **40**, 38 (1968).
- ⁷⁵ Z. Hendrikse, M. Elout, and W. Maaskant, Computer Physics Communications **86**, 297 (1995).